14q32 Noncoding RNAs in vascular remodelling

Goossens, E.A.C.

Chapter 3

Genetic associations and regulation of expression indicate an independent role for 14q32 snoRNAs in human cardiovascular disease

Cardiovascular Research 2019 Aug 1;115(10):1519-1532

EAC Goossens[1,2] *
KEJ Hakansson[1,2] *
S Trompet[3,4] *
E van Ingen[1,2]
MR de Vries[1,2]
RVCT van der Kwast[1,2]
RS Ripa[5]
J Kastrup[5]
PJ Hohensinner[6]
C Kaun[6]
J Wojta[6]
S Böhringer[7]
S Le Cessie[7,8]
JW Jukema[3]
PHA Quax[1,2]
AY Nossent[1,2,9]

* Authors contributed equally to this work

[1]Department of Surgery and [2]Einthoven Laboratory for Experimental Vascular Medicine, Leiden University Medical Center, Leiden, The Netherlands; [3]Department of Cardiology, Leiden University Medical Center, Leiden, the Netherlands; [4]Department of Gerontology and Geriatrics, Leiden University Medical Center, Leiden, the Netherlands; [5]Department of Cardiology, Rigshospitalet University of Copenhagen, Copenhagen, Denmark; [6]Department of Internal Medicine II, Medical University of Vienna, Vienna, Austria; [7]Department of Biomedical Data Sciences, Leiden University Medical Center, Leiden, the Netherlands; [8]Department of Clinical Epidemiology, Leiden University Medical Center, Leiden, the Netherlands; and [9]Ludwig Boltzmann Cluster for Cardiovascular Research, Vienna, Austria

Abstract

Aims: We have shown that 14q32 microRNAs are highly involved in vascular remodelling and cardiovascular disease. However, the 14q32 locus also encodes 41 'orphan' small nucleolar RNAs (snoRNAs). We aimed to gather evidence for an independent role for 14q32 snoRNAs in human cardiovascular disease.

Methods and results: We performed a lookup of the 14q32 region within the dataset of a genome wide association scan in 5244 participants of the PROspective Study of Pravastatin in the Elderly at Risk (PROSPER). Single nucleotide polymorphisms (SNPs) in the snoRNA-cluster were significantly associated with heart failure. These snoRNA-cluster SNPs were not linked to SNPs in the microRNA-cluster or in MEG3, indicating that snoRNAs modify the risk of cardiovascular disease independently. We looked at expression of 14q32 snoRNAs throughout the human cardio-vasculature. Expression profiles of the 14q32 snoRNAs appeared highly vessel specific. When we compared expression levels of 14q32 snoRNAs in human vena saphena magna (VSM) with those in failed VSM-coronary bypasses, we found that 14q32 snoRNAs were up-regulated. SNORD113.2, which showed a 17-fold up-regulation in failed bypasses, was also up-regulated two-fold in plasma samples drawn from patients with ST-elevation myocardial infarction directly after hospitalization compared with 30 days after start of treatment. However, fitting with the genomic associations, 14q32 snoRNA expression was highest in failing human hearts. *In vitro* studies show that the 14q32 snoRNAs bind predominantly to methyl-transferase Fibrillarin, indicating that they act through canonical mechanisms, but on non-canonical RNA targets. The canonical C/D-box snoRNA seed sequences were highly conserved between humans and mice.

Conclusions: 14q32 snoRNAs appear to play an independent role in cardiovascular pathology. 14q32 snoRNAs are specifically regulated throughout the human vasculature and their expression is up-regulated during cardiovascular disease. Our data demonstrate that snoRNAs merit increased effort and attention in future basic and clinical cardiovascular research.

Introduction

Noncoding RNAs (ncRNAs) are a booming topic of research. Formerly seen as 'junk RNA', ncRNAs have been shown to be important regulators of gene expression. Of all ncRNAs, microRNAs have been studied most extensively over the past decade. MicroRNAs bind the 3'UTR of their target messenger RNA (mRNA) to inhibit translation[1]. The fact that microRNAs can fine-tune expression levels of large sets of target genes, up to several hundred genes per microRNA, makes them attractive therapeutic targets for multifactorial pathophysiological processes, including cardiovascular disease. We have recently discovered that a large gene cluster of 54 microRNAs transcribed from the long arm of human chromosome 14 (14q32) is highly involved in cardiovascular pathology[2,3]. Inhibition of individual 14q32 microRNAs led to increases in post-ischaemic blood flow recovery and tissue perfusion in mice via increased neovascularization[4]. At the same time, inhibition of these microRNAs also decreased plasma cholesterol and atherosclerotic lesion formation, whereas increasing plaque stability in atherosclerosis-prone mice[5].

Besides 54 microRNAs, the human 14q32 locus also encodes genes for two other types of ncRNAs, namely three long noncoding RNAs (lncRNAs) and 41 small nucleolar RNAs (snoRNAs). Interestingly, one of these lncRNAs, MEG3, was found to be up-regulated in activated endothelial cells under hypoxia[6] and play a role in angiogenesis[7]. LncRNAs have caught the attention of many research groups. Even though their mechanisms-of-action are still poorly understood, the number of publications on lncRNAs in cardiovascular disease is increasing exponentially[8–19]. SnoRNAs on the other hand are still relatively unknown and understudied. Like microRNAs, snoRNAs are a class of highly conserved small ncRNA molecules[20]. SnoRNAs are typically between 60 nucleotides and 300 nucleotides long and can be divided into two subtypes. 'H/ACA box' snoRNAs modulate other ncRNAs via pseudouridylation. 'C/D box' snoRNAs modulate ncRNAs via 2'O-ribose-methylation. However, snoRNAs have also been found to act via non-canonical pathways. SnoRNAs influence metabolic stress, lipotoxicity, and intracellular cholesterol trafficking, independent of their canonical function[21,22]. Moreover, there are snoRNAs that have no known RNA targets at all. These snoRNAs most likely have mostly non-canonical functions and are referred to as 'orphan snoRNAs'. All 14q32 snoRNAs are orphan snoRNAs of the C/D box subtype[23]. With the increasing research attention for lncRNAs, we aimed to investigate whether orphan snoRNAs merit similar attention. First, we found significant associations of genetic variations specifically in the snoRNA region of the 14q32 locus with human cardiovascular disease. Second, we observed differential expression of 14q32 snoRNA levels throughout the human vasculature. And third, we demonstrate that snoRNA expression is regulated during cardiovascular disease, both in vascular tissue samples and in plasma, as

well in a murine model for vein graft disease. Overall, our data demonstrate that snoRNAs indeed merit similar effort and attention in future basic and clinical cardiovascular research as microRNAs and lncRNAs do.

Methods

PROspective study of pravastatin in the elderly at risk

PROspective study of pravastatin in the elderly at risk (PROSPER) was a prospective multicentre randomized placebo-controlled trial to assess whether treatment with pravastatin diminishes the risk of major vascular events in elderly[24]. Between December 1997 and May 1999, we screened and enrolled subjects in Scotland (Glasgow), Ireland (Cork), and the Netherlands (Leiden). Men and women aged 70–82 years were recruited if they had pre-existing vascular disease or increased risk of such disease because of smoking, hypertension, or diabetes. A total number of 5804 subjects were randomly assigned to pravastatin or placebo. The protocol meets the criteria of the Declaration of Helsinki and was approved by the medical ethics committees of each participating institution. Written informed consent was obtained from all participating subjects. All data have been anonymized.

The primary endpoint in the study was the combined endpoint of death from coronary heart disease, non-fatal myocardial infarction (MI), and occurrence of clinical stroke, either fatal or non-fatal. When death occurred following a non-fatal stroke within a period of 28 days, it was regarded as a fatal stroke. Secondary endpoints were the separate coronary and cerebrovascular components of the primary endpoint. Heart failure hospitalization was a tertiary endpoint. All endpoints were adjudicated by the study endpoint committee. More details about the diagnosis of the cerebrovascular and coronary events within the PROSPER study has been published elsewhere[25]. A whole genome wide screening had been performed in the sequential PHASE project[26]. Of 5763 subjects, DNA was available for genotyping. Genotyping was performed with the Illumina 660K beadchip, after QC (call rate <95%) 5244 subjects and 557 192 single nucleotide polymorphism (SNPs) were left for analysis. These SNPs were imputed to 2.5 million SNPs based on the HAPMAP build 36withMACH imputation software. For this study, we performed a candidate gene study. We extracted all SNPs within the genomic region of the 14q32 cluster from the 2.5 million SNP database with use of the PLINK software (http://pngu.mgh.harvard.edu/~purcell/plink/download.shtml#download).

As confirmation of our findings, data on associations between 14q32 SNPs and coronary artery disease/MI have been contributed by CARDIoGRAMplusC4D investigators and have been downloaded from http://www.cardiogramplusc4d.org.

Collection of human vascular tissues

Human vascular tissue samples, including vena saphena magna (VSM) samples, were collected during general surgery for various implications. Only surplus material, discarded after surgery, was collected and stored at -80°C. Failed coronary bypasses were collected during autopsy, formalin-fixed, and paraffin-embedded.

All samples were anonymized and no data were recorded that trace back to an individual's identity. Collection, storage, and processing of the samples were performed in compliance with the Medical Treatment Contracts Act (WGBO, 1995) and the Code of Conduct for Health Research using Body Material (Good Practice Code, Dutch Federation of Biomedical Scientific Societies, 2002) and the Dutch Personal Data Protection Act (WBP, 2001).

Human plasma samples

From a Danish cohort study on G-CSF treatment in ST-elevation myocardial infarction (STEMI) patients[27], 23 placebo-treated STEMI patients (21 men, two women) aged 54 ± 8 years (mean ± standard deviation) who had been treated successfully with primary percutaneous coronary intervention within 12 h after symptom onset were included in our study. STEMI was diagnosed from typical angina for more than 30min, the presence of ST-elevations >0.4mV in at least two contiguous leads on a standard 12-lead ECG and a significant rise in MI serum markers. Further inclusion criteria included age between 20 years to 70 years, a proximal lesion in a coronary artery branch and either serum creatine kinase-MB above 100IL/L or significant Q-wave development. Patients were excluded if they had a prior MI, significant non-culprit stenosis, ventricular arrhythmia after percutaneous coronary intervention, pregnancy, diagnosed, or suspected cancer, New York Heart Association class 3–4 heart failure symptoms or severe claustrophobia.

Blood samples were drawn from the antecubital vein using EDTA-coated tubes. Samples were kept on ice and processed within 30min after collection. Plasma was obtained from the samples by centrifugation at 3000g for 10min, with the plasma closest to the buffy coat being discarded. After centrifugation, the plasma samples were aliquoted and stored at -80°C until analysis.

The study was approved by the ethics committee at Rigshospitalet, Copenhagen, Denmark (KF 01-239/02). All patients received oral and written information about the study, and written informed consent was obtained before inclusion in the study, which conformed to the Declaration of Helsinki.

Collection of human heart failure tissues

Biopsies were collected from explanted end-stage failing human hearts, caused by dilatory cardiomyopathy (N= 9), ischaemic cardiomyopathy (N= 6), right ventricular dysplasia (N= 1), or congenital heart disease (N= 2). Samples were collected from both the apex and the affected ventricle. As we found no differences, average expression levels from the apex and ventricles were used for each patient in further analyses. All human material was obtained and processed according to the recommendations of the hospital's ethics committee and security board, including informed consent and in accordance with the Declaration of Helsinki. RNA was isolated from heart tissue using an automated Maxwell System with the respective mRNA tissue kit (Promega, WI, USA). cDNA was generated from equal amounts of RNA per experiment using a Promega GoScript reverse transcription system (Promega).

Murine vein graft model

All animal experiments have been approved by the Leiden University Medical Center animal ethics committee (Dier Ethische Commissie) and all animal procedures were performed conform to the guidelines from Directive 2010/63/EU of the European Parliament on the protection of animals used for scientific purposes. Male ApoE3*Leiden mice, aged 10weeks to 20weeks were housed with water and chow ad libitum. Mice were fed a western-type diet (ABdiets), which resulted in plasma cholesterol levels between 12mmol/L and 24mmol/L, as determined before surgery and after surgery (Roche Diagnostics).

Vein graft surgery was performed by donor caval vein interpositioning (caval vein of ~2mm length) in the carotid artery of recipient mice[28]. Before surgery, mice were anaesthetized with midazolam (5mg/kg, Roche Diagnostics), medetomidine (0.5mg/kg, Orion), and fentanyl (0.05mg/kg, Janssen Pharmaceutical). The adequacy of the anaesthesia was monitored by keeping track of the breathing frequency and the response to toe pinching of the mice. After the procedure, the mice were antagonized with atipamezol (2.5mg/kg, Orion) and fluminasenil (0.5mg/kg Fresenius Kabi). Buprenorphine (0.1mg/kg, MSD Animal Health) was given after surgery to relieve pain. Mice were sacrificed after 3 days, 7 days, 14 days, or 28 days (four mice per time point) by exsanguination under anaesthesia; 12 untransplanted caval veins were collected as time point 0; three caval veins were pooled yielding four samples. The vein grafts and caval veins were removed and snap frozen.

RNA isolation and rt/qPCR

Fresh-frozen human vascular tissue samples and murine vein graft/caval vein were submerged in liquid nitrogen and homogenized by use of pestle and mortar. After complete evaporation of the liquid nitrogen, total RNA was isolated by standard TRIzol-chloroform

extraction. From cells, the medium was removed and cells were washed in PBS, after which the cells were lysed in TRIzol and RNA isolated by standard TRIzol-chloroform extraction. From paraffin embedded human coronary bypasses, total RNA was isolated using the RNeasy FFPE Kit according to manufacturer's protocol (Qiagen). From human plasma samples, total RNA from 100µL of plasma was extracted using the miRCURY RNA Isolation Kit—Biofluids (Exiqon) according to manufacturer's protocol, including rDNase treatment to prevent DNA contamination. RNA quantity and purity were checked using nanodrop (Nanodrop® Technologies).

RNA was reverse transcribed using 'high-capacity RNA to cDNA kit' (ThermoFisher) and quantified by qPCR using SybrGreen reagents (Qiagen) on the VIIa7 (ThermoFisher). SnoRNA expression was normalized against U6 alone or U6 and GAPDH together, to warrant reference gene stability over samples, using the 2^{-dCt} method. Human snoRNA primer sequences were taken from a study by Valleron et al[29]. Although the snoRNAs and U6 could be reliably and reproducibly measured in RNA isolated from paraffin-embedded human failed coronary bypass tissues, longer RNAs, including MEG3, MEG8, could not, most likely due to degradation of longer RNAs by RNases. Shorter RNAs are protected from RNase digestion, as they are in complex with RNA Binding Proteins[30]. All qPCR primers used are given in Supplementary data, Table S5.

Isolation of human umbilical venous and arterial endothelial cells, arterial smooth muscle cells, and arterial fibroblasts

Umbilical cords were collected from full-term pregnancies and stored in sterile PBS at 4°C and subsequently used for cell isolation within 7 days. For human umbilical venous endothelial cell/human umbilical arterial endothelial cell (HUVEC/HUAEC) isolation, a cannula was inserted in the umbilical vein or in one of the umbilical arteries and flushed with sterile PBS. The vessels were infused with 0.075% collagenase Type II (Worthington, Lakewood, NJ, USA) and incubated at 37°C for 20min. The collagenase solution was collected and the vessels were flushed with PBS in order to collect all detached endothelial cells. The cell suspensions were centrifuged at 400g for 5min, and the pellet was resuspended in HUVEC/HUAEC culture medium [M199 (PAA, Pasching, Austria), 10% heat inactivated human serum (PAA), 10% heat inactivated newborn calf serum (PAA), 1% penicillin/streptomycin (MP Biomedicals, Solon, OH, USA), 150mg/mL endothelial cell growth factor (kindly provided by Dr Koolwijk, VU Medical Center, Amsterdam, the Netherlands), and 0.1% heparin (LEO Pharma, Ballerup Danmark)]. HUAECs were cultured in plates coated with 1% gelatin.

The second artery was removed and cleaned from remaining connective tissue. Endothelial cells were removed by gently rolling the artery over a blunted needle. The tunica adventitia and tunica media were separated using surgical forceps. After overnight incubation in human umbilical arterial smooth muscle cell/human umbilical arterial fibroblast (HUASMC/HUAF) culture medium [DMEM GlutaMAX™ (Invitrogen, GIBCO, Auckland, New Zealand), 10% heat inactivated foetal bovine serum (PAA), 10% heat inactivated human serum, 1% penicillin/streptomycin, and 1% non-essential amino acids (PAA)], both tunicae were incubated separately in a 2mg/mL collagenase Type II solution (Worthington) at 37°C. Cell suspensions were filtered over a 70 mm cell strainer and centrifuged at 400 g for 10min. Cell pellets were resuspended and plated in culture medium. Cells isolated from the tunica adventitia were washed with culture medium after 90 min to remove slow-adhering non-fibroblast cells.

Primary cell culture

Cells were cultured at 37°C in a humidified 5% CO_2 environment. Culture medium was refreshed every 2–3 days. Cells were passed using trypsin-EDTA (Sigma, Steinheim, Germany) at 90–100% (HUVECs, HUAECs, and HUASMCs) or 70–80% confluency (HUAFs). HUVECs, HUASMCs, and HUAFs were used up to passage six and HUAECs up to passage three. Stock solutions of isolated HUVECs, HUASMCs, and HUAFs up to passage four, and HUAECs up to passage two were stored at -180°C in DMEM GlutaMAX™ containing 20% FBS and 10% DMSO (Sigma).

3T3 cell culture

3T3 cells were cultured at 37°C under 5% CO_2. Cells were grown in DMEM (PAA) with high glucose and stable L-glutamine, supplemented with 10% foetal calf serum and penicillin/streptomycin.

Primary mouse fibroblasts culture

Murine primary fibroblasts were isolated from ear-clippings of 3-week old C57BL/6 mice. Ear clippings were cut into small pieces, which were embedded in 0.2% gelatin in 10 cm2 plates and covered in DMEM supplemented with 20% FCSi and 1% NEAA for approximately 7 days, cells were expanded to passage 3 and frozen down in liquid nitrogen for later use. Fibroblasts from P4 were trypsinized and passed into 12-wells plates for scratch-wound healing assays. Cells were used up to passage P5–P7.

RBP-immunoprecipitation

For RNA binding protein (RBP)-immunoprecipitation (RIP), either HUAFs or 3T3 cells were grown to 70–80% confluence in T-175 culture flasks, one flask per RBP-pull-down, in normal culture medium. We used the EZ-Magna RIP RNA-Binding Protein Immunoprecipitation Kit (Merck-Millipore) for cell lysis, sample preparation and RBP-pull-down, according to manufacturer's protocol. We used antibodies against SNRP70 (provided with EZ-Magna RIP kit), Dicer, AGO1, Fibrillarin, and a negative control IgG (all by Abcam) for RBP-pull-down. RNA was isolated using standard TRIzol-chloroform extraction and snoRNA expression was measured by rt/qPCR as described above. Expression was normalized to expression in a 10% input sample, using the 2^{-dCt} method; after cell lysis, but before RBP-pull-down, 10% (100 mL) of each lysate was collected and used for RNA extraction directly.

SnoRNA upregulation in vitro and scratch-wound healing assay

Primary murine fibroblasts were seeded in 12-well plates at 50 000 cells per well in normal culture medium. The next day, cells were incubated with 10ng/mL 3rd generation antisense molecules (3GAs) in medium with 0.5% foetal calf serum for 24 h. Sequences of all 3GAs used are given in Supplementary data, Table S4. After 24 h, medium was aspirated and a scratch-wound was made across the diameter of each well using a p200 pipet tip. Next, cells were washed with PBS, and fresh low serum medium containing 3GAs was added. In order to monitor wound closure, live phase-contrast microscopy (Axiovert 40C, Carl Zeiss) was used for taking pictures immediately after (0 h) and 12 h after introducing the scratch-wound. Pictures were taken at two different locations in each well and averaged for analysis. Scratch size was calculated at 0 h and 12 h using the wound healing tool macro for ImageJ. Finally, cells were washed with PBS and TRIzol was added for RNA isolation.

Statistical analyses

For the candidate gene study, logistic regression was used to associate the 14q32 SNPs with cardiovascular outcomes adjusted for sex, age, country, and pravastatin treatment. All statistical analyses were performed with PLINK statistical software (http://pngu.mgh.harvard.edu/~purcell/plink/download.shtml#download). P-values <0.05 were considered statistically significant.

SNPs were pruned based on linkage, using LDLink software (https://analysistools.nci.nih.gov/LDlink/)[31,32]. For pruning, we used the CEU population as reference which corresponds to the PROSPER population (r^2= 0.3, MAF= 0.01).We performed correction for multiple testing, using both Bonferroni and false discovery rate (FDR) corrections within each gene region of the 14q32 locus, as our a priori interest lays

with the snoRNA gene region and the other regions were included to allow for correction of potential confounding by linkage. An FDR of 10% was chosen. We also performed correction for multiple testing on the pruned SNPs in the locus as a whole with a global test, using the tail strength method, including all genes in the 14q32 locus, looking at associations with heart failure. The tail strength measures how much P-values in a set differ from the expected uniform distribution under the null hypothesis and sums up these differences into single-test statistics[33]. We used a cutoff of 10% and 20% for missingness in individuals and markers, respectively. The global P-value was calculated using a logistic regression model on each SNP and summarizing the P-values using the tail strength. To account for residual LD between SNPs, 10^4 permutations were used to derive an empirical P-value. R version 3.5.0 was used for all calculations.

Normalized relative expression levels of noncoding RNAs expressed as mean + SEM. Differences between groups were assessed using student's t-tests. Because of large inter-sample variation, a Grubbs' test was used to identify significant outliers ($\alpha < 0.05$) in human 14q32 ncRNA expression levels, resulting in exclusion of three individual measurements. In the STEMI samples, the variance over time was analyzed using repeated measures one-way analyses of variance (ANOVA). Tukey's range test was used as a *post hoc* test to find significant variation between two measurement time points.

For *in vitro* assays two-tailed Student's t-tests or two-way ANOVA were used to compare groups. A level of P-value <0.05 was considered significant. A Grubbs' test was used to identify significant outliers ($\alpha = 0.05$), resulting in exclusion of two individual scratch assays. However, the data still include a minimum of three independent experiments for each snoRNA.

Results

Association of 14q32 genetic variations with cardiovascular disease

The 14q32 locus is depicted in Figure 1. To establish a role of 14q32 snoRNAs in human cardiovascular disease, we focused on SNPs in the 14q32 locus that were genotyped in 5244 participants of the PROSPER study. Characteristics of PROSPER participants are given in Supplementary data, Table S1, all data on extracted 14q32 SNPs are given in the Supplementary data, Data S2 file. When zooming in on the different genes in the locus, six SNPs in the protein coding gene DLK1 were included, of which one associated with coronary events; 53 SNPs in the lncRNA MEG3 gene were included, of which eight associated with cardiovascular endpoints; seven SNPs in the lncRNA MEG8 gene were included, of which one associated with heart failure; and 11 SNPs in the lncRNA MEG9 gene were included of which three associated with vascular mortality and two with all-cause mortality. In the two regions that encode the vast majority of the snoRNAs and microRNAs within the locus, 51 and 42 SNPs were included in the array, respectively, of which 17 and 13 associated with cardiovascular endpoints and of these, 14 and 9 SNPs, respectively, associated with heart failure (Figure 2).

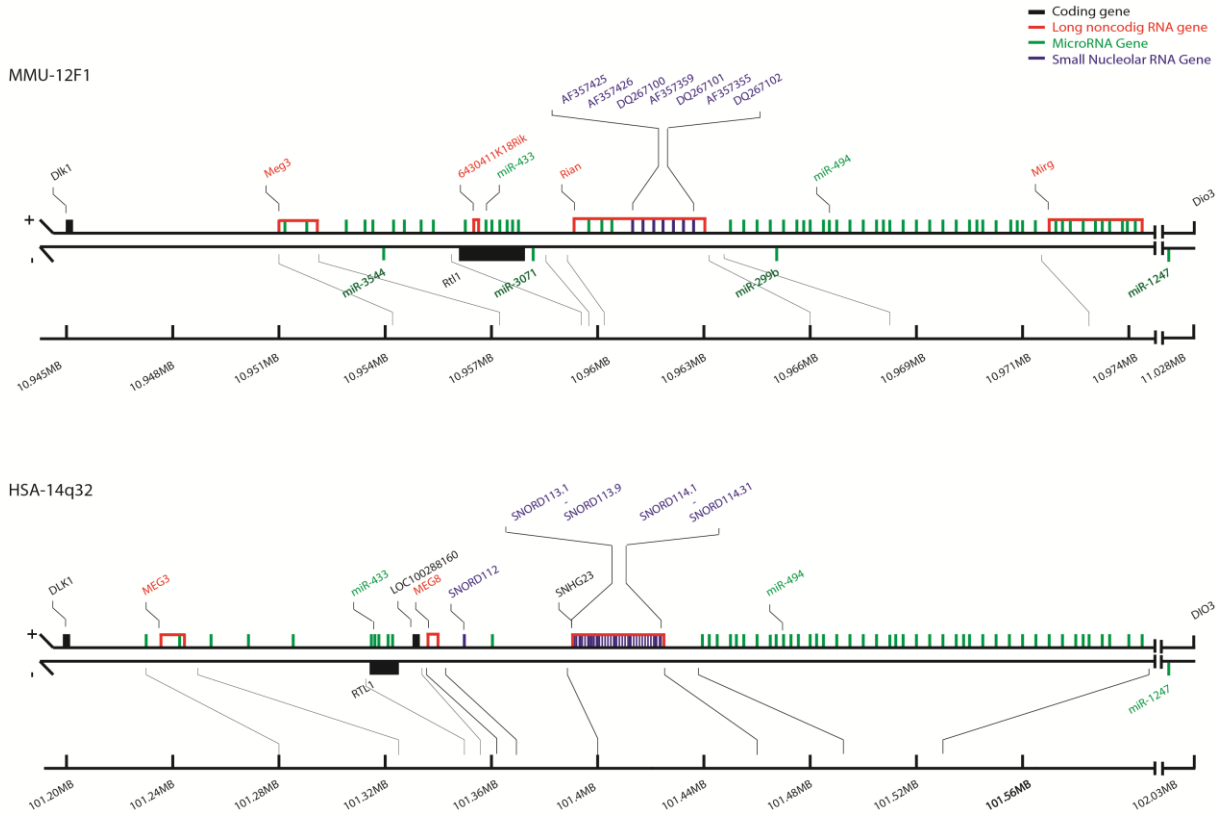

Figure 1 Schematic representation of the imprinted human 14q32 and murine 12F1 loci. Protein coding genes are depicted in black, lncRNA genes in red, microRNA genes in green, and snoRNA genes in blue.

We then pruned SNPs based on linkage, to correct for multiple testing. For DLK1, MEG3, RTL1, MEG8, the snoRNA region, the microRNA region, and MEG9, 6, 17, 3, 4, 8, 14, and 2 SNPs were kept, respectively. Data on kept and pruned SNPs per gene are given in the Supplementary data, Data S3 file. After Bonferroni correction per gene, one SNP in the snoRNA region (rs2145501) was significantly associated with heart failure. After FDR correction per gene, four SNPs in the snoRNA region were significantly associated with heart failure (rs2145501, rs2145504, rs2295657, and rs10133948). After both Bonferroni and FDR correction per gene, two SNPs in the MEG9 gene (rs2295655 and rs3742406) were significantly associated with vascular mortality and one SNP with all-cause mortality (rs2295655). The odds ratios, P-values, and corrected P-value thresholds are shown in Supplementary data, Table S2B. Multiple correction testing data on all pruned SNPs per gene are given in the Supplementary data, Data S4 file.

We also performed a global test on SNPs kept after pruning using the tail strength method to correct for multiple testing over the locus as a whole, looking at associations with heart failure. The global P-value was 0.018, meaning that the null-hypothesis of no associated SNPs in the locus is rejected and that the 14q32 locus associates significantly with heart failure.

SNPs in the locus were selected from a genome wide screening array dataset, in which SNPs are selected more or less evenly over the length of the genome and preferably in coding sequences. Since there are no coding sequences on the positive strand of the 14q32 locus, except for DLK1, none of the SNPs included in the analyses were located directly in a snoRNA gene. Therefore, we rely on the fact that SNPs that are located in proximity of each other are often inherited together, also referred to as linkage. Non-functional SNPs can be associated with cardiovascular endpoints because they are linked to a different, functional SNP. We determined r^2 values, a measure of linkage between SNPs. We found evidence of linkage within the MEG3 gene, within the microRNA-cluster, and within the snoRNA-cluster, which underlines their individual biological importance. However, we also found that there was virtually no linkage between the SNPs in the snoRNA-cluster and those in the microRNA-cluster. In fact, there is a recombination hotspot in between both clusters. There is another recombination hotspot between MEG3 and the snoRNA-cluster, as well as one between the microRNA-cluster and MEG9. This is in fact a crucial finding, because it demonstrates that the 14q32 snoRNAs associate with cardiovascular endpoints, independently of the microRNAs and MEG3 (Supplementary data, Figure S1A–C). A more detailed view of linkage within the snoRNA-cluster is given in Supplementary data, Figure S2.

As confirmation of our genetic association data, we performed a lookup of 14q32 SNPs in the publicly available meta-analysis dataset of cardiogram (www.cardiogramplusc4d.org). To our knowledge, public data on heart failure specifically are not available yet, but cardiogram focuses on coronary artery disease. All extracted cardiogram data are provided in the Supplementary data, Data S5 file, and significant associations directly in (the vicinity of) 14q32 noncoding RNA genes are given in Supplementary data, Table S6.

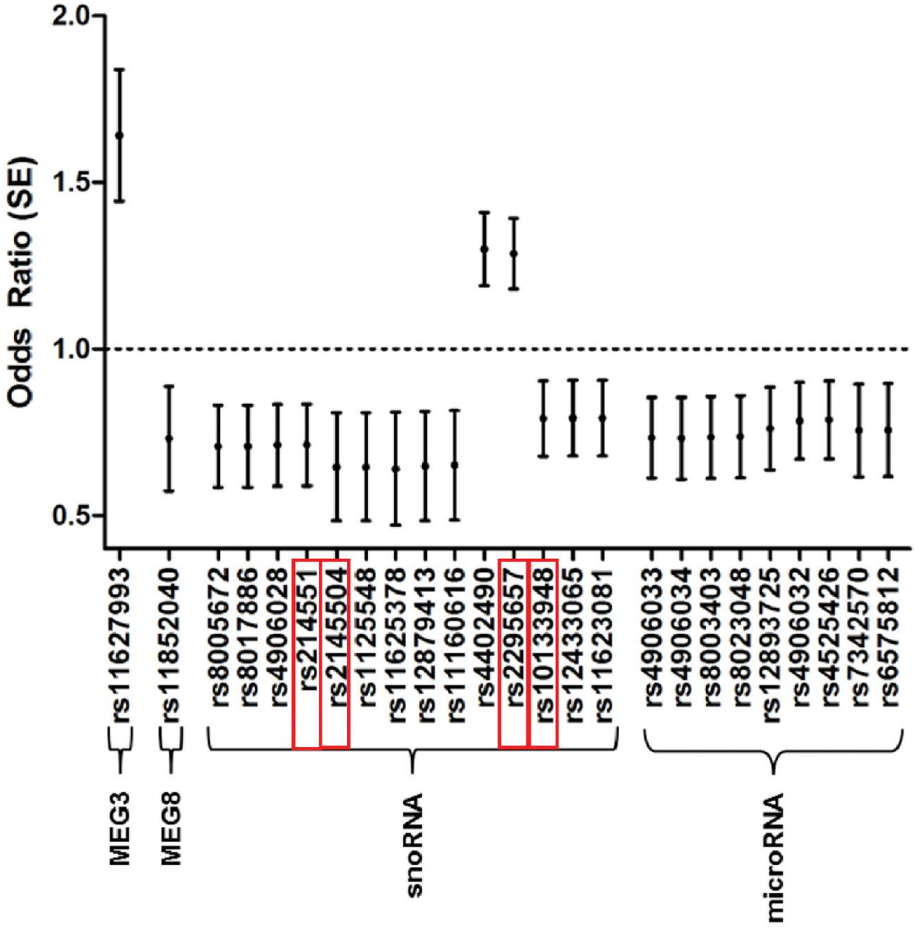

Figure 2 14q32 SNPs and heart failure. Odds ratios, ± standard errors, are given of SNPs that associate significantly with heart failure. SNPs are given in order of their chromosomal location and accolades indicate their respective regions in the 14q32 locus. Only the four SNPs outlined in red remain significant after correction for multiple testing.

Global expression of 14q32 snoRNAs

The cluster contains three highly related copy-sets of SNORD112 (one copy), SNORD113 (nine copies) and SNORD114 (31 copies). Since the snoRNAs are highly similar in sequences, rt/qPCR primers can only reliably discriminate 7 of the 41 snoRNAs, namely SNORD112, SNORD113.2, SNORD113.6, SNORD113.7, SNORD113.8, SNORD113.9, and SNORD114.1. We measured these seven snoRNAs in a biobank of 95 human vascular tissue samples, collected

during general surgery within the LUMC (Supplementary data, Table S3). With the exception of SNORD113.2, all measured 14q32 snoRNAs were abundantly expressed throughout the vasculature (Supplementary data, Figure S3A–G). Global snoRNA expression was highest however in the arteries and veins of the head and neck, again with the exception of SNORD113.2, which was expressed most abundantly in vessels of the lower limbs and in mammarian arteries (Figure 3).

Samples were collected during general surgery for any indication. However, most vessels were collected during vascular surgery for peripheral artery disease and coronary artery bypass grafting on the one hand or tumour resections on the other. However, none of the snoRNAs were differentially expressed between benign and perimalignant vessels. Nor did snoRNA expression associate with age or sex (data not shown).

We also assessed 14q32 snoRNA expression in four types of human primary vascular cells, isolated from the umbilical cord, namely HUVECs, HUAECs, HUASMCs, and HUAFs. Although we observed consistent snoRNA expression in all four cell types, expression was clearly enriched in HUASMCs (Supplementary data, Figure S4).

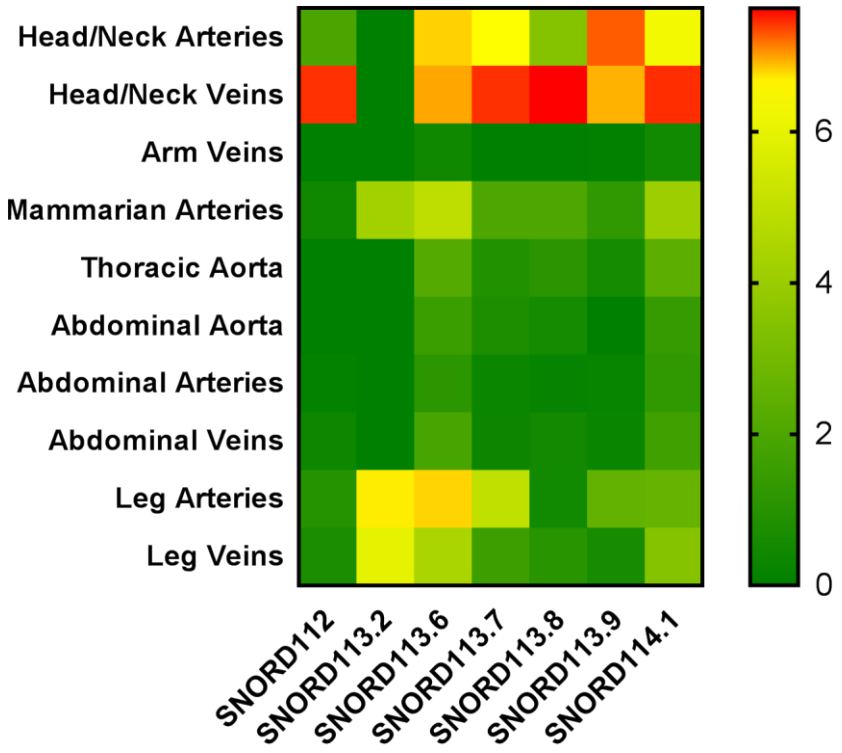

Figure 3 Heatmap of snoRNA expression in human vasculature. SnoRNAs are grouped in vessel origin and in order of their genetic localization. For every snoRNA, relative expression, calculated using the 2^{-dCt} method, in each vessel group was normalized against the average expression in all samples. Relative expression below average is green, around average is yellow, and above average is orange to red. The total number of vessels included was 95.

14q32 snoRNA expression in failed human coronary arterial-venous bypass grafts

We compared 14q32 snoRNA expression in naive VSMs and failed arterial-venous bypasses. Naïve VSMs were harvested during bypass surgery and served as 'baseline' controls for failed coronary arterial-venous bypass grafts. In failed bypasses, expression levels of 14q32 snoRNAs SNORD112 and SNORD113.6 remained more or less stable. Expression levels of SNORD113.2, SNORD113.7, SNORD113.8, SNORD113.9, and SNORD114.1 on the other hand appeared upregulated between two-fold and 20-fold (Figure 4A–G).

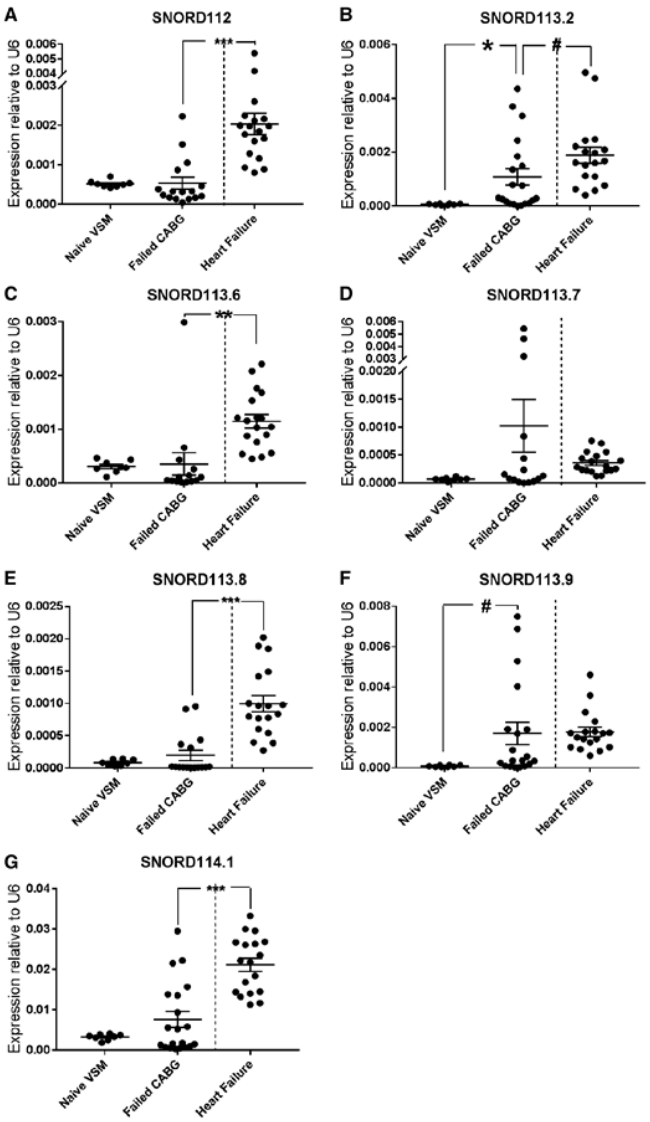

Figure 4 Regulation of the 14q32 small ncRNAs in human vein graft disease and expression in human failing hearts (A–G). Relative expression, calculated using the 2^{-dCt} method, of 14q32 microRNAs and snoRNAs in failed coronary bypasses (right bars; N= 20), compared with naive vena saphena magna harvested during bypass surgery (left bars; N= 8), as well as expression levels in human end-stage failing hearts (N= 18). Mean values are given and errors bars represent SEMs. #P<0.1; *P<0.05; **P<0.01; ***P<0.001 (t-test).

14q32 snoRNA expression in end-stage failing human hearts

As we observed the strongest association between SNPs in the snoRNA region and heart failure, we also looked at snoRNA expression in tissue samples from explanted end-stage failing human hearts. For obvious reasons, we had no healthy heart tissue samples for comparison. However, as shown in Figure 4A–G, all measured 14q32 snoRNAs were expressed in failing human hearts. When compared with expression in failing bypass grafts, expression was higher in heart failure samples for five out seven measured snoRNAs [SNORD112: 3.8-fold (P> 0.001); SNORD113.2: 1.7-fold (P = 0.07); SNORD113.6: 3.2-fold (P> 0.01); SNORD113.8: 5.1-fold (P> 0.001); and SNORD114.1: 2.8-fold (P < 0.001), and similar for the remaining SNORD113.7 (P = 0.13) and SNORD113.9 (P=0.91)].

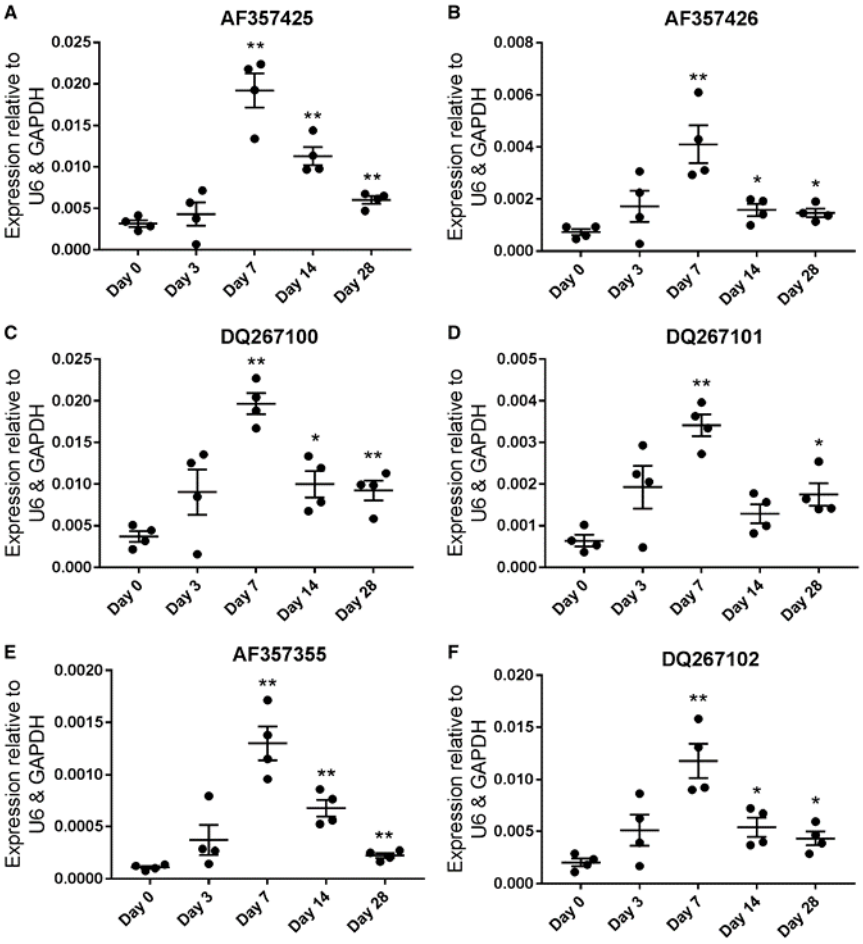

Figure 5 Regulation of the 12F1 snoRNAs in murine vein grafts (A–F). Relative expression, calculated using the 2^{-dCt} method, over time, relative to naive venae cavae, in vein grafts in ApoE*3L mice. Mean values are given and errors bars represent SEMs. *P<0.05; **P<0.01 (t-test). Each time point includes vein grafts from four mice, except for time point 0, which contains four pools of naive caval veins from three mice (12 mice in total).

Murine snoRNA expression in a model for arteriovenous bypass failure

The 14q32 noncoding RNA cluster is conserved in eutheria and is transcribed from the imprinted 12F1 locus in mice (Figure 1).We compared expression of six different 12F1 snoRNAs in murine vein grafts, a model for arterial-venous bypass failure. Expression of all 12F1 snoRNAs increases after vein graft surgery and peaks at 7 days after vein grafting. After 7 days, levels decrease, but they do not normalize and remain elevated until Day 28 (Figure 5).

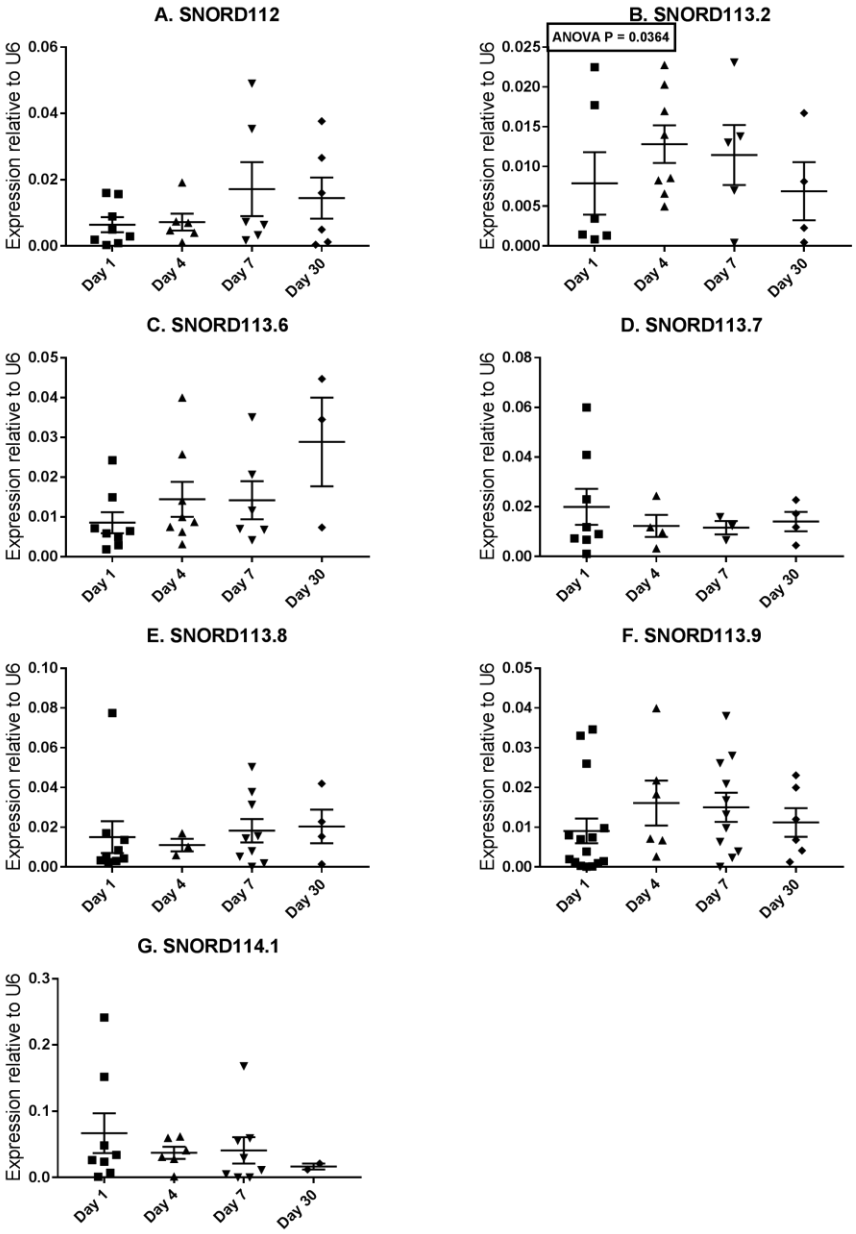

Figure 6 Regulation of circulating 14q32 snoRNA expression (A–G). Relative expression, calculated using the 2^{-dCt} method, of 14q32 snoRNAs, in plasma of patients with STEMI, collected over time. Mean values are given and errors bars represent SEMs. P-value for ANOVA is given for SNORD113.2. Although 23 patients were included in all measurements, some snoRNAs remained below detection levels in some patient samples.

14q32 circulating snoRNAs in ST-elevation myocardial infarction

In our STEMI-patient cohort, we measured the same seven 14q32 snoRNAs in plasma, drawn at hospitalization, and on Day 4, Day 7, and Day 30 after hospitalization. All seven snoRNAs could be detected in plasma, albeit in low levels (some snoRNAs remained below the detection limit in some individuals). SNORD113.2 levels were regulated over time in response to STEMI [P= 0.0364; F(3,22) = 3.381]. SNORD113.2 levels were increased two-fold between Day 4 and Day 30 (P = 0.0424), suggesting a sub-acute increased expression at Day 4 in comparison to the assumed normal expression levels at Day 30 (Figure 6B). Remaining snoRNAs appeared regulated over time as well but significant changes in expression were not observed (Figure 6A and C–G).

Potential mechanisms of action

To gain more insight into the potential role of 14q32 snoRNAs in cardiovascular pathology, we looked at different aspects of snoRNA biology. We performed RIP in both human and murine cells to determine which RBPs can bind the 14q32/12F1 snoRNAs. We found no evidence of snoRNA-binding to the spliceosome in either human or murine cells (SNRNP70; data not shown). In primary human umbilical arterial adventitial fibroblasts (HUAAFs), all 14q32 snoRNAs measured were bound to Fibrillarin and to a lesser extent also to AGO1. Binding to Fibrillarin was consistent and outspoken for all 14q32 snoRNAs measured, even though expression of SNORD113.2 was relatively low in all fractions, including the whole-cell lysate (10% input) (Figure 7A). 14q32 snoRNAs were clearly enriched in the Fibrillarin fraction compared to the Fibrillarin target U6 (U6 is a snRNA that methylated by Fibrillarin), even though U6 expression in human fibroblasts is approximately 1000-fold higher than 14q32 snoRNA expression (Supplementary data, Figure S4).

The murine 12F1 snoRNAs did not bind to Ago1, but all 12F1 snoRNAs, with the exception of DQ267101, were clearly enriched in the Fibrillarin fraction (Figure 7B). Fibrillarin is the methyltransferase that performs snoRNA-directed 2'O-ribose-methylation of target ncRNAs. Therefore, these data indicate that 14q32/12F1 snoRNAs direct 2'O-ribose-methylation via Fibrillarin of non-canonical RNA targets. Furthermore, 14q32 snoRNAs may interact with the microRNA processor protein AGO1.

3GAs [formerly known as Gene Silencing Oligonucleotides (GSOs)], which have proven very reliable in microRNA-inhibition[4], proved less efficient as snoRNA-inhibitors; 3GAs directed towards the 5'-end of the snoRNA knocked-down snoRNA expression by 40–80% (data not shown). SnoRNAs have proven notoriously difficult to inhibit, likely due to their predominantly nucleolar localization and more complex structures[34]. However, 3GAs directed to the 3'-end lead to up-regulation of all 12F1 snoRNAs, except for AF3574276,

which showed virtually no expression in murine fibroblasts (Figure 7C). SnoRNAs are processed by exonucleases[35,36] and 3GA-binding to the 3'-end may protect against exonuclease digestion.

We then used 3'-end-directed 3GAs to overexpress the 12F1 snoRNAs individually in mouse fibroblasts and performed scratch wound healing assays to assess changes in proliferation and migration. Upregulation of snoRNA AF357425 led to a significantly impaired scratch wound healing (32% reduction compared with 3GA-Control, P= 0.0065), whereas up-regulation of snoRNA DQ267102 showed a similar trend (19% reduction compared with 3GA-Control, P=0.083) (Figure 7D).

snoRNA conservation

So far, only seven 12F1 snoRNAs have been annotated in mice vs. 41 14q32 snoRNAs in humans (NCBI Gene). However, 19 more murine 12F1 snoRNAs have been predicted based on sequence, but have not been confirmed as existing snoRNAs yet (UCSC Genome Browser). We were able to design unique rt/qPCR primers for 16 of the 19 additional predicted murine snoRNAs and measured their potential expression in murine fibroblasts (Supplementary data, Figure S5). Not only were these 16 snoRNAs all expressed, but also at a higher level than the seven annotated snoRNAs. rt/qPCR is not a confirmative experiment to demonstrate that these sequences are mature snoRNAs, we could pick up remaining Rian pre-lncRNA, or not yet degraded Rian introns. However, it is feasible that the murine 12F1 locus is more closely related to the human 14q32 locus in snoRNA abundance than previously assumed. We then aligned the sequences of the human and murine snoRNAs and, although there are overlapping regions, there also was large variability. However, if we assume that these snoRNAs function via Fibrillarin, then we know the 'seed sequences' of the snoRNAs, namely the nine nucleotides upstream of the D-boxes. If we align these, we observed clearly conserved seed sequences of murine and human snoRNAs (Supplementary data, Figure S6). Specifically, murine snoRNAs (names starting with AF, DQ, or GM) cluster with human snoRNAs (names starting with SNORD) based on sequence, rather than with other murine snoRNAs and vice versa. Furthermore, the alternative seed sequences, the nine nucleotides upstream of potential D'-boxes, are also largely conserved.

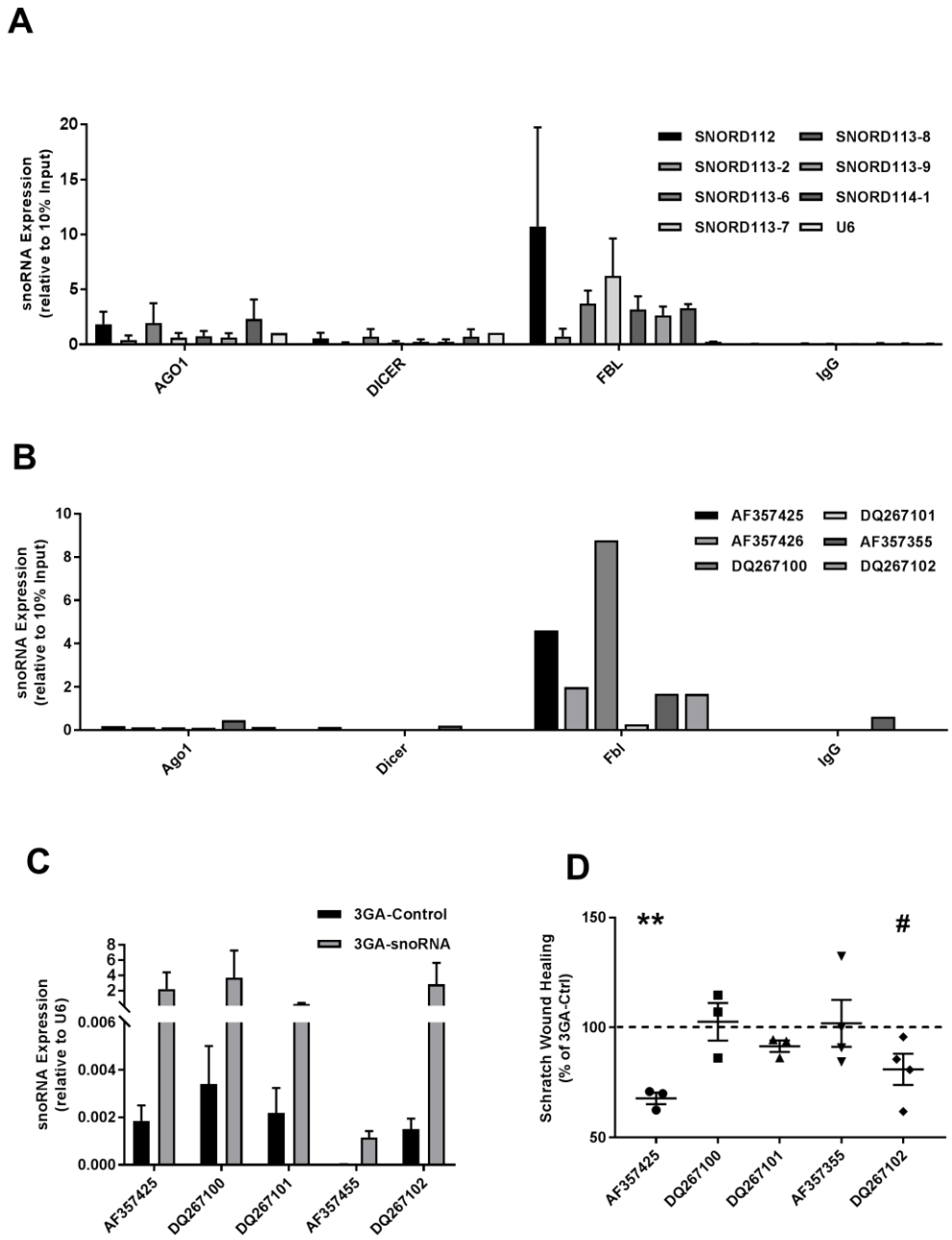

Figure 7 Functionality screenings on 14q32 and 12F1 snoRNAs. (A) RIP, followed by RNA isolation and rt/qPCR on primary HUAAFs. Expression levels of each snoRNA were normalized to snoRNA expression in untreated cell lysates (input) using the 2^{-dCt} method. IgG pull-down was used as negative control. The data represent three independent experiments performed in triplicate. (B) RIP, followed by RNA isolation and rt/qPCR on the murine fibroblast 3T3 cell line. Expression levels of each snoRNA were normalized to snoRNA expression in untreated cell lysates (input) using the 2^{-dCt} method. IgG pulldown was used as negative control. The data represent technical triplicates. (C) *In vitro* up-regulation of snoRNAs using 3'-end-directed 3GAs in murine primary fibroblasts. Expression levels were normalized to U6 using the 2^{-dCt} method. (D) Scratch-wound healing in primary murine fibroblasts at 12 h after scratch-wound placement. Data are presented as mean% of 3GA-Control ± SEM. #P< 0.1 and **P< 0.01 compared with 3GA-Control (t-test). Each data point represents an independent experiment performed in triplicate.

Discussion

In the present study, we have gathered evidence for an independent role of orphan snoRNAs in cardiovascular disease. First, we demonstrated significant associations of SNPs in the 14q32 snoRNA locus with cardiovascular events in a large population-based study. Second, we showed differential expression of 14q32 snoRNAs throughout the human vasculature. And third, we show regulation of 14q32 snoRNAs, in human tissue samples and in human plasma after cardiovascular disease. The 14q32 microRNAs and lncRNAs have previously been implied in cardiovascular pathology. However, here we uncover evidence that the 14q32 orphan snoRNAs play an independent role in cardiovascular disease for the first time.

Such an individual and independent role of 14q32 snoRNAs in cardiovascular disease was supported by our findings in our candidate gene study performed in the PROSPER study. Not only did we find the highest density of significantly associated SNPs of all 14q32 regions in the snoRNA-cluster, the fact that there are recombination hotspots that separate the snoRNA-region from the MEG3 and microRNA-cluster in the 14q32 locus also strongly implies an independent role of 14q32 snoRNAs in cardiovascular pathology. After correction for multiple testing per gene, only four SNPs in the snoRNA-region, as well two SNPs in the more remote MEG9 gene, remained significantly associated with cardiovascular endpoints. The snoRNA-SNPs associated specifically with heart failure. Even though we have no comparison to healthy human heart tissue, we do show that the 14q32 snoRNAs are abundantly expressed in the failing human heart.

However, we must keep in mind that on the used genome wide screening arrays, SNPs are selected preferably in coding sequences, and thus, none of the SNPs included in our analyses was located directly within a snoRNA gene itself. With the revolution of ncRNA research, it appears that we have stumbled upon an unexpected weakness in all the large genomic studies that have been performed in recent years, as most noncoding regions have been excluded or at least understudied.

We have previously described a regulatory role for several 14q32 microRNAs in vascular remodelling, in neovascularization, as well as in atherosclerosis and restenosis[4,5,37]. We also found that 14q32 microRNAs are regulated in distinct temporal expression patterns during vascular remodelling and that both the microRNA's temporal regulation, as well as its basal expression levels, is independent of its genomic location within the cluster. Looking at the 14q32 snoRNAs, we found a similar phenomenon. For example, even though all the snoRNAs are processed from adjacent introns of the SNHG23 host gene, SNORD113.2 showed very distinct expression patterns throughout the vasculature. Furthermore, the 14q32 snoRNAs showed differential regulation after both vein graft failure and after STEMI.

These findings indicate a leading role for posttranscriptional regulation processes in 14q32 snoRNA expression. However, they also indicate individual roles for all 14q32 snoRNAs in vascular remodelling and cardiovascular disease. Thus, whether or not a snoRNA is regulated during cardiovascular disease appears independent of its genomic location, but maybe dependent on its function instead.

Perhaps our best clues about these functions and about the mechanisms-of-action of orphan snoRNAs come from a highly similar ncRNA cluster, located on human locus 15q11. Like the 14q32 locus, the 15q11 cluster is imprinted. The locus also encodes multiple ncRNA genes, including two copy sets of orphan C/D box snoRNAs, SNORD115 (48 copies), and SNORD116 (29 copies). Deletions in the 15q11 locus cause Prader–Willi syndrome, which is characterized by cognitive disabilities, low muscle tone, short stature, incomplete sexual development, and a chronic feeling of hunger that can lead to morbid obesity. It is believed that the snoRNAs, particularly SNORD116, play a major role in Prader–Willi pathology. Studies have shown that 15q11 orphan snoRNAs can influence mRNA expression levels of over 200 genes, as well as each other's[38]. The 15q11 snoRNAs have been shown to direct alternative splicing of target mRNAs as well as influence mRNA editing[39,40]. In exploratory experiments, we did not find evidence of 14q32 snoRNA interactions with the spliceosome, even though this does not fully exclude a function for 14q32 snoRNAs in alternative splicing. However, we did find that both the human 14q32 snoRNAs and the murine 12F1 snoRNAs bind to predominantly to Fibrillarin, the canonical 2'O-ribose-methyltransferase associated with C/D box snoRNAs. Furthermore, the canonical snoRNA seed sequences, the nine nucleotide directly upstream of the C- and D'-boxes are highly conserved between the human 14q32 and murine 12F1 snoRNAs. This implies that 14q32 snoRNAs direct 2'O-ribose-methylation of their target RNAs and that their target-set, rather than their mechanism-of-action, is noncanonical. 2'O-ribose-methylation can protect RNAs from editing[40], which would fit with the findings for the 15q11 cluster.

Partial deletions and loss of imprinting also occur in the 14q32 locus and lead to a broad range of different pathologies. However, cluster-wide deletions are embryonically lethal. Interestingly, knockout of 12F1 lncRNA Meg3 in mice led to over-expression of several pro-angiogenic genes, including VEGF and DLL4, and to a drastically increased vascular capillary density in mouse embryos[41].

Besides alternative splicing and mRNA-editing, two other functions have been described for orphan snoRNAs. Some snoRNAs, like many lncRNAs, may function as competitive endogenous RNAs (ceRNAs), where they compete for binding of a microRNA with the microRNA's target mRNAs[42]. Other snoRNAs are processed into smaller RNAs and loaded into the RNA-induced silencing complex, where they function as snoRNA-derived microRNAs

and inhibit translation of their own set of target mRNAs[43]. We found that most human 14q32 snoRNAs indeed interact with the microRNA-processor as they also bind to AGO1. The binding to AGO1 could indicate a microRNA-like function; however, it is more likely that snoRNAs direct 2'O-ribose methylation of precursor microRNAs, via binding to the 2'O-ribose methyl-transferase Fibrillarin, as we recently showed that microRNAs are subject to Fibrillarin-dependent 2'O-ribose methylation[44]. This hypothesis is strengthened by the fact that the snoRNA seed sequences are conserved between mice and humans. Conservation in snoRNA seed sequences, implies conservation in the snoRNAs' target RNAs. MicroRNAs are one of the highest conserved RNA species. Therefore, it is plausible that the 14q32 snoRNAs target microRNAs, rather than rRNAs or snRNAs.

In summary, we have collected multiple lines of evidence for an independent role of 14q32 orphan snoRNAs in cardiovascular disease. Genetic variations in the 14q32 snoRNA-cluster are significantly associated with cardiovascular events, 14q32 snoRNAs are differentially expressed throughout the human vasculature and 14q32 snoRNA expression levels are regulated during cardiovascular disease. Therefore, we advocate that snoRNAs merit similar attention as other ncRNAs, such as microRNAs and lncRNAs, in future basic and clinical research, both within the field of cardiovascular disease and in other fields of research.

Acknowledgements

We thank Daphne van den Homberg for technical support. We kindly acknowledge Sudhir Agrawal and Idera Pharmaceuticals for the design and supply of the 3GAs.

References

1. Bartel DP. MicroRNAs: genomics, biogenesis, mechanism, and function. Cell 2004; 116:281–297.
2. Nossent AY, Eskildsen TV, Andersen LB, Bie P, Bronnum H, Schneider M, Andersen DC, Welten SM, Jeppesen PL, Hamming JF, Hansen JL, Quax PH, Sheikh SP. The 14q32 microRNA-487b targets the antiapoptotic insulin receptor substrate 1 in hypertension-induced remodeling of the aorta. Ann Surg 2013;258:743–751.
3. Welten SM, Goossens EA, Quax PH, Nossent AY. The multifactorial nature of microRNAs in vascular remodelling. Cardiovasc Res 2016;110:6–22.
4. Welten SM, Bastiaansen AJ, de JR, de Vries MR, Peters EH, Boonstra M, Sheikh SP, La MN, Kandimalla ER, Quax PH, Nossent AY. Inhibition of 14q32 MicroRNAs miR-329, miR-487b, miR-494 and miR-495 increases neovascularization and blood flow recovery after ischemia. Circ Res 2014;115:696–708.
5. Wezel A, Welten SM, Razawy W, Lagraauw HM, de Vries MR, Goossens EA, Boonstra MC, Hamming JF, Kandimalla ER, Kuiper J, Quax PH, Nossent AY, Bot I. Inhibition of MICRORNA-494 reduces carotid artery atherosclerotic lesion development and increases plaque stability. Ann Surg 2015;262:841–847; discussion 847–848.
6. Michalik KM, You X, Manavski Y, Doddaballapur A, Zornig M, Braun T, John D, Ponomareva Y, Chen W, Uchida S, Boon RA, Dimmeler S. Long noncoding RNA MALAT1 regulates endothelial cell function and vessel growth. Circ Res 2014;114:1389–1397.
7. Boon RA, Hofmann P, Michalik KM, Lozano-Vidal N, Berghäuser D, Fischer A, Knau A, Jae´ N, Schu¨rmann C, Dimmeler S. Long noncoding RNA Meg3 controls endothelial cell aging and function: implications for regenerative angiogenesis. J Am Coll Cardiol 2016;68:2589–2591.
8. Busch A, Eken SM, Maegdefessel L. Prospective and therapeutic screening value of non-coding RNA as biomarkers in cardiovascular disease. Ann Transl Med 2016;4:236.
9. Dechamethakun S, Muramatsu M. Long noncoding RNA variations in cardiometabolic diseases. J Hum Genet 2016;62:97–104.
10. Lorenzen JM, Thum T. Long noncoding RNAs in kidney and cardiovascular diseases. Nat Rev Nephrol 2016;12:360–373.
11. Ballantyne MD, McDonald RA, Baker AH. lncRNA/MicroRNA interactions in the vasculature. Clin Pharmacol Ther 2016;99:494–501.
12. Creemers EE, van Rooij E. Function and therapeutic potential of noncoding RNAs in cardiac fibrosis. Circ Res 2016;118:108–118.
13. Archer K, Broskova Z, Bayoumi AS, Teoh JP, Davila A, Tang Y, Su H, Kim IM. Long non-coding RNAs as master regulators in cardiovascular diseases. Int J Mol Sci 2015; 16:23651–23667.
14. Ounzain S, Burdet F, Ibberson M, Pedrazzini T. Discovery and functional characterization of cardiovascular long noncoding RNAs. J Mol Cell Cardiol 2015;89:17–26.
15. Devaux Y, Zangrando J, Schroen B, Creemers EE, Pedrazzini T, Chang CP, Dorn GW, Thum T, Heymans S. Long noncoding RNAs in cardiac development and ageing. Nat Rev Cardiol 2015;12:415–425.
16. Philippen LE, Dirkx E, da Costa-Martins PA, de Windt LJ. Non-coding RNA in control of gene regulatory programs in cardiac development and disease. J Mol Cell Cardiol 2015;89:51–58.
17. Thum T, Condorelli G. Long noncoding RNAs and microRNAs in cardiovascular pathophysiology. Circ Res 2015;116:751–762.
18. Uchida T, Wada H, Mizutani M, Iwashita M, Ishihara H, Shibano T, Suzuki M, Matsubara Y, Soejima K, Matsumoto M, Fujimura Y, Ikeda Y, Murata M. Identification of novel mutations in ADAMTS13 in an adult patient with congenital thrombotic thrombocytopenic purpura. Blood 2004;104:2081–2083.
19. Boon RA, Jae N, Holdt L, Dimmeler S. Long noncoding RNAs: from clinical genetics to therapeutic targets? J Am Coll Cardiol 2016;67:1214–1226.

20. Kiss T. Small nucleolar RNA-guided post-transcriptional modification of cellular RNAs. EMBO J 2001;20:3617–3622.
21. Brandis KA, Gale S, Jinn S, Langmade SJ, Dudley-Rucker N, Jiang H, Sidhu R, Ren A, Goldberg A, Schaffer JE, Ory DS. Box C/D small nucleolar RNA (snoRNA) U60 regulates intracellular cholesterol trafficking. J Biol Chem 2013;288:35703–35713.
22. Michel CI, Holley CL, Scruggs BS, Sidhu R, Brookheart RT, Listenberger LL, Behlke MA, Ory DS, Schaffer JE. Small nucleolar RNAs U32a, U33, and U35a are critical mediators of metabolic stress. Cell Metab 2011;14:33–44.
23. Cavaille J, Seitz H, Paulsen M, Ferguson-Smith AC, Bachellerie JP. Identification of tandemly-repeated C/D snoRNA genes at the imprinted human 14q32 domain reminiscent of those at the Prader-Willi/Angelman syndrome region. Hum Mol Genet 2002;11:1527–1538.
24. Shepherd J, Blauw GJ, Murphy MB, Bollen EL, Buckley BM, Cobbe SM, Ford I, Gaw A, Hyland M, Jukema JW, Kamper AM, Macfarlane PW, Meinders AE, Norrie J, Packard CJ, Perry IJ, Stott DJ, Sweeney BJ, Twomey C, Westendorp RG. Pravastatin in elderly individuals at risk of vascular disease (PROSPER): a randomised controlled trial. Lancet 2002;360:1623–1630.
25. Shepherd J, Blauw GJ, Murphy MB, Cobbe SM, Bollen EL, Buckley BM, Ford I, Jukema JW, Hyland M, Gaw A, Lagaay AM, Perry IJ, Macfarlane PW, Meinders AE, Sweeney BJ, Packard CJ, Westendorp RG, Twomey C, Stott DJ. The design of a prospective study of pravastatin in the elderly at risk (PROSPER). PROSPER Study Group. PROspective study of pravastatin in the elderly at risk. Am J Cardiol 1999;84:1192–1197.
26. Trompet S, de Craen AJ, Postmus I, Ford I, Sattar N, Caslake M, Stott DJ, Buckley BM, Sacks F, Devlin JJ, Slagboom PE, Westendorp RG, Jukema JW. Replication of LDL GWAs hits in PROSPER/PHASE as validation for future (pharmaco)genetic analyses. BMC Med Genet 2011;12:131.
27. Ripa RS, Jorgensen E, Wang Y, Thune JJ, Nilsson JC, Sondergaard L, Johnsen HE, Kober L, Grande P, Kastrup J. Stem cell mobilization induced by subcutaneous granulocyte-colony stimulating factor to improve cardiac regeneration after acute ST-elevation myocardial infarction: result of the double-blind, randomized, placebocontrolled stem cells in myocardial infarction (STEMMI) trial. Circulation 2006;113:1983–1992.
28. Simons KH, Peters HAB, Jukema JW, de Vries MR, Quax PHA. A protective role of IRF3 and IRF7 signalling downstream TLRs in the development of vein graft disease via type I interferons. J Intern Med 2017;282:522–536.
29. Valleron W, Laprevotte E, Gautier EF, Quelen C, Demur C, Delabesse E, Agirre X, Prosper F, Kiss T, Brousset P. Specific small nucleolar RNA expression profiles in acute leukemia. Leukemia 2012;26:2052–2060.
30. Mitchell PS, Parkin RK, Kroh EM, Fritz BR, Wyman SK, Pogosova-Agadjanyan EL, Peterson A, Noteboom J, O'Briant KC, Allen A, Lin DW, Urban N, Drescher CW, Knudsen BS, Stirewalt DL, Gentleman R, Vessella RL, Nelson PS, Martin DB, Tewari M. Circulating microRNAs as stable blood-based markers for cancer detection. Proc Natl Acad Sci USA 2008;105:10513–10518.
31. Machiela MJ, Chanock SJ. LDlink: a web-based application for exploring populationspecific haplotype structure and linking correlated alleles of possible functional variants. Bioinformatics 2015;31:3555–3557.
32. Machiela MJ, Chanock SJ. LDassoc: an online tool for interactively exploring genomewide association study results and prioritizing variants for functional investigation. Bioinformatics 2018;34:887–889.
33. Taylor J, Tibshirani R. A tail strength measure for assessing the overall univariate significance in a dataset. Biostatistics 2005;7:167–181.
34. Ploner A, Ploner C, Lukasser M, Niederegger H, Huttenhofer A. Methodological obstacles in knocking down small noncoding RNAs. RNA 2009;15: 1797–1804.

35. Cavaille J, Bachellerie JP. Processing of fibrillarin-associated snoRNAs from premRNA introns: an exonucleolytic process exclusively directed by the common stembox terminal structure. Biochimie 1996;78:443–456.
36. Kiss T, Filipowicz W. Exonucleolytic processing of small nucleolar RNAs from premRNA introns. Genes Dev 1995;9:1411–1424.
37. Welten SMJ, de Jong RCM, Wezel A, de Vries MR, Boonstra MC, Parma L, Jukema JW, van der Sluis TC, Arens R, Bot I, Agrawal S, Quax PHA, Nossent AY. Inhibition of 14q32 microRNA miR-495 reduces lesion formation, intimal hyperplasia and plasma cholesterol levels in experimental restenosis. Atherosclerosis 2017;261:26–36.
38. Falaleeva M, Surface J, Shen M, de la Grange P, Stamm S. SNORD116 and SNORD115 change expression of multiple genes and modify each other's activity. Gene 2015;572:266–273.
39. Kishore S, Khanna A, Zhang Z, Hui J, Balwierz PJ, Stefan M, Beach C, Nicholls RD, Zavolan M, Stamm S. The snoRNA MBII-52 (SNORD 115) is processed into smaller RNAs and regulates alternative splicing. Hum Mol Genet 2010;19:1153–1164.
40. Vitali P, Basyuk E, Le ME, Bertrand E, Muscatelli F, Cavaille J, Huttenhofer A. ADAR2-mediated editing of RNA substrates in the nucleolus is inhibited by C/D small nucleolar RNAs. J Cell Biol 2005;169:745–753.
41. Gordon FE, Nutt CL, Cheunsuchon P, Nakayama Y, Provencher KA, Rice KA, Zhou Y, Zhang X, Klibanski A. Increased expression of angiogenic genes in the brains of mouse meg3-null embryos. Endocrinology 2010;151:2443–2452.
42. Taulli R, Pandolfi PP. "Snorkeling" for missing players in cancer. J Clin Invest 2012;122: 2765–2768.
43. Ender C, Krek A, Friedlander MR, Beitzinger M, Weinmann L, Chen W, Pfeffer S, Rajewsky N, Meister G. A human snoRNA with microRNA-like functions. Mol Cell 2008;32:519–528.
44. van der Kwast R, van Ingen E, Parma L, Peters HAB, Quax PHA, Nossent AY. Adenosine-to-inosine editing of microRNA-487b alters target gene selection after ischemia and promotes neovascularization. Circ Res 2018;122:444–456.

Supplementary data

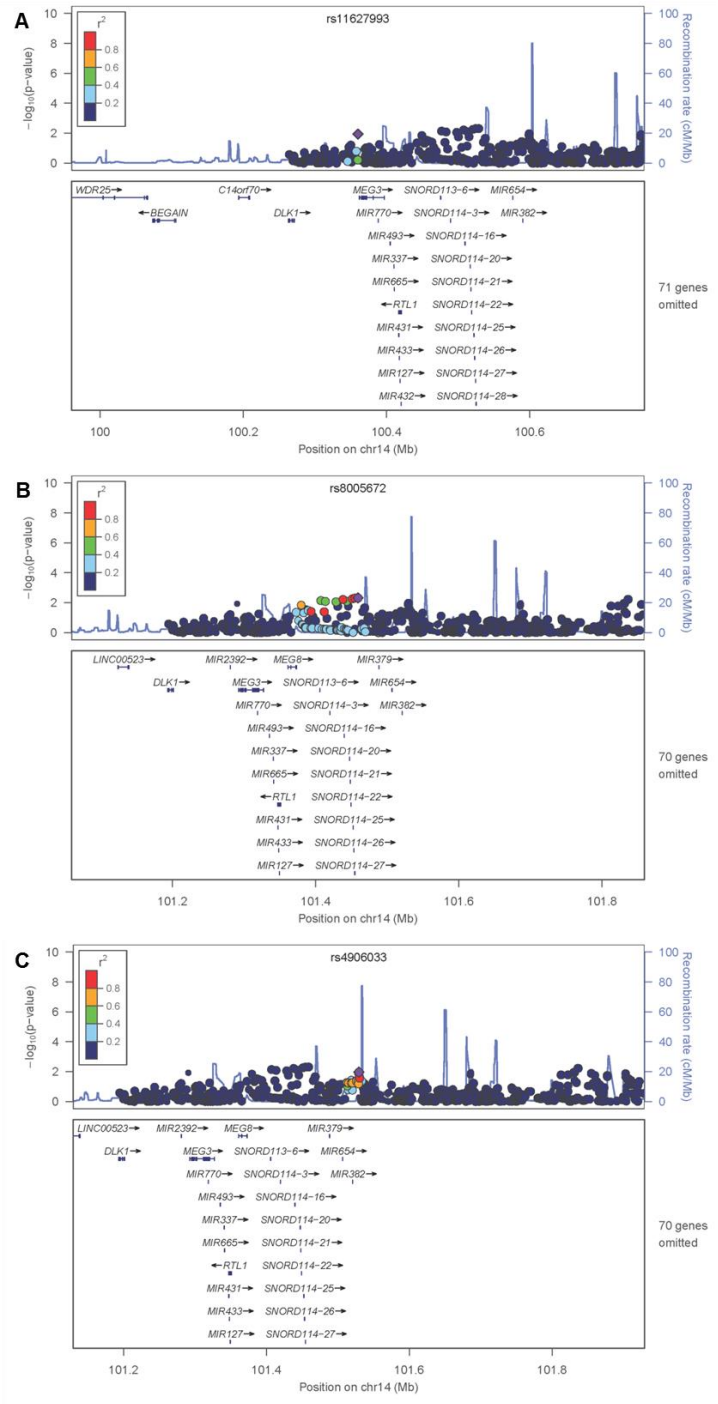

Supplemental Figure 1 Linkage of selected SNPs in *MEG3*, the snoRNA and microRNA clusters of the 14q32 locus. (A-C) Locuszoom images of r^2-values for SNPs in the *MEG3* (rs11627993), snoRNA (rs8005672) and microRNA (rs4906033) regions, respectively. The p-values correspond to the association between the SNPs and Heart Failure. Blue peaks represent recombination hotspots.

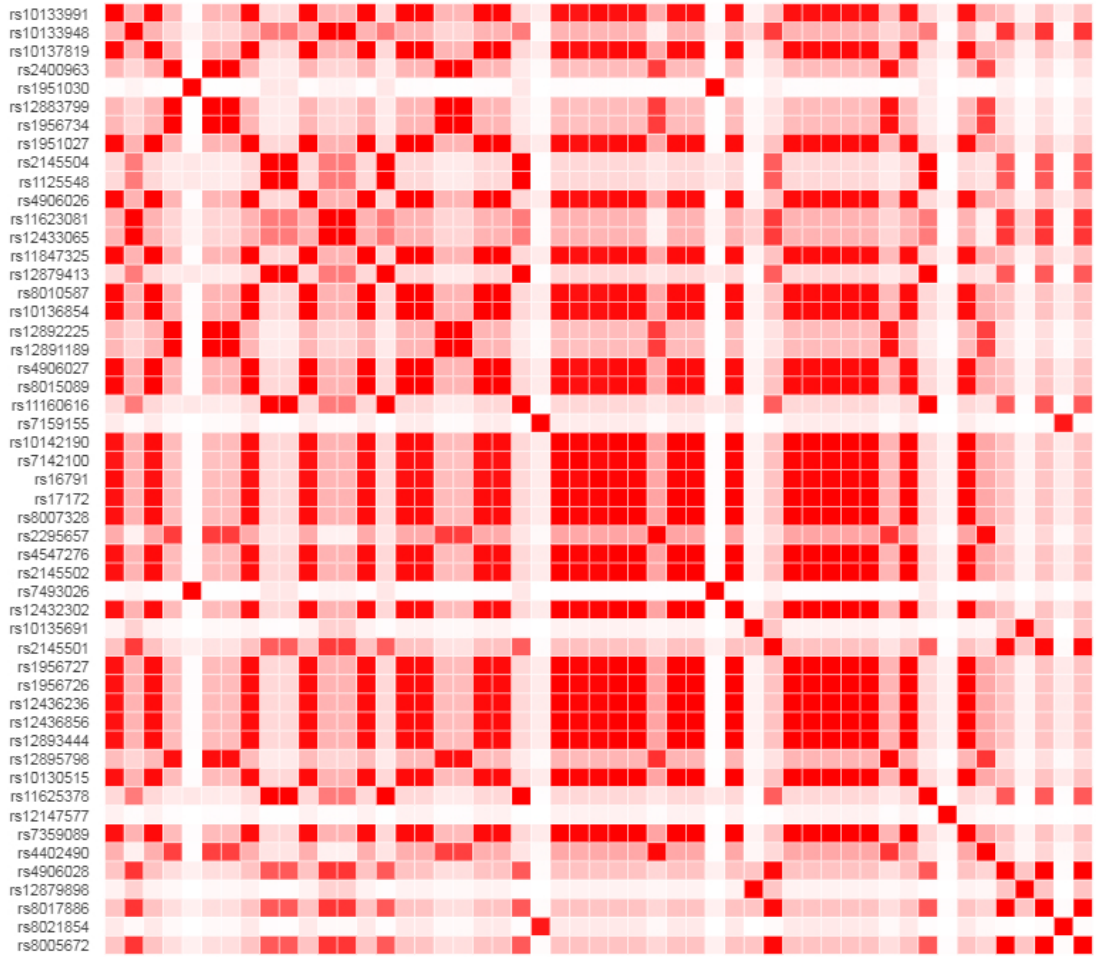

Supplemental Figure 2 Linkage between SNPs in the snoRNA cluster in the CEU-population. The same SNPs, in the same order, are placed on the X-axis as on the Y-axis. Linkage, expressed as r^2, is shown as a gradient from red to white, where red squares represent two SNPs that are in full linkage-disequilibrium and white squares represent two SNPs that are not linked at all.

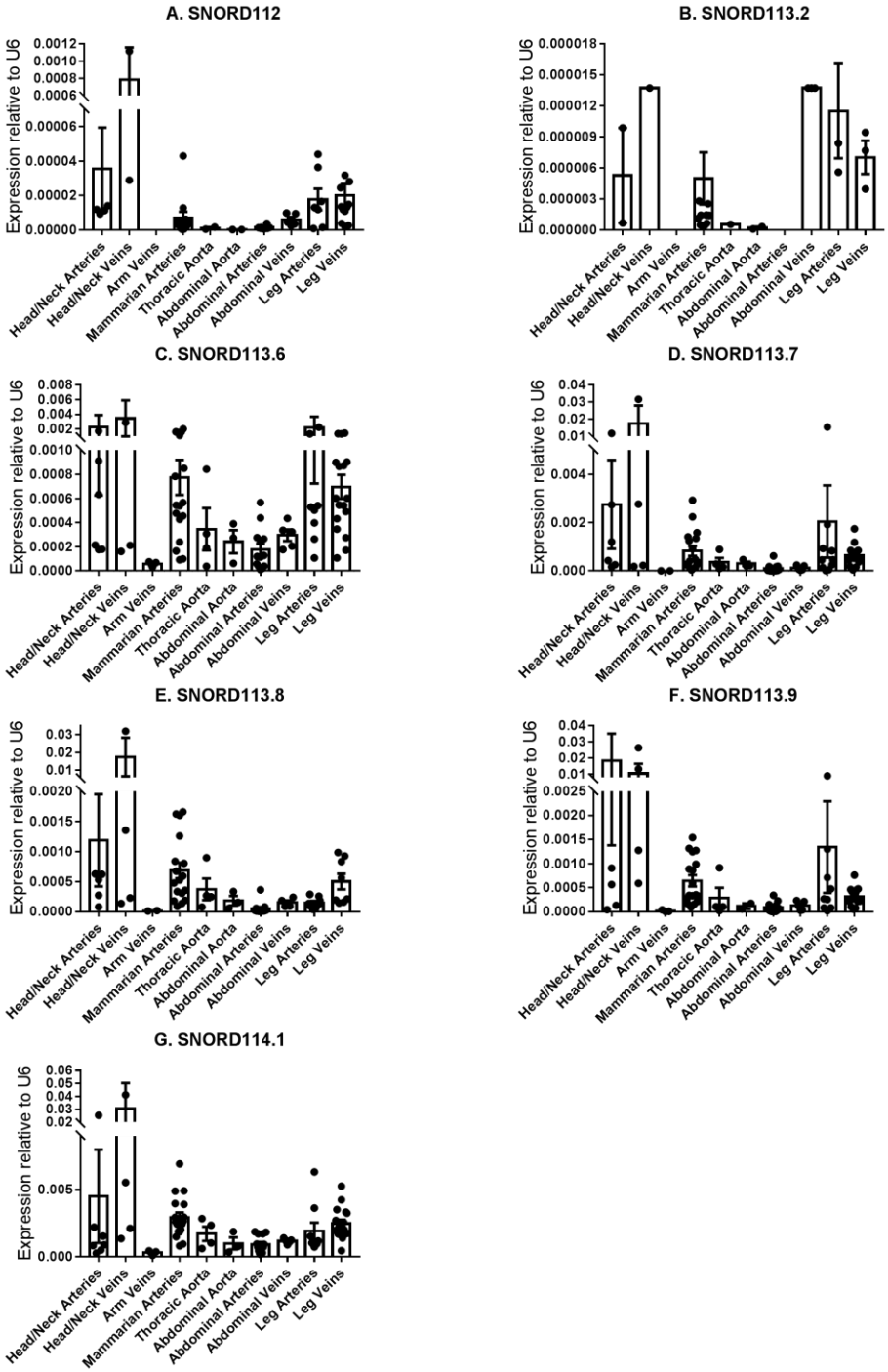

Supplemental Figure 3 Expression profiles of 14q32 snoRNAs throughout the human vasculature. Mean values are given and errors bars represent SEMs. U6 expression was used for normalization using the $2^{-\Delta Ct}$ method. N=95.

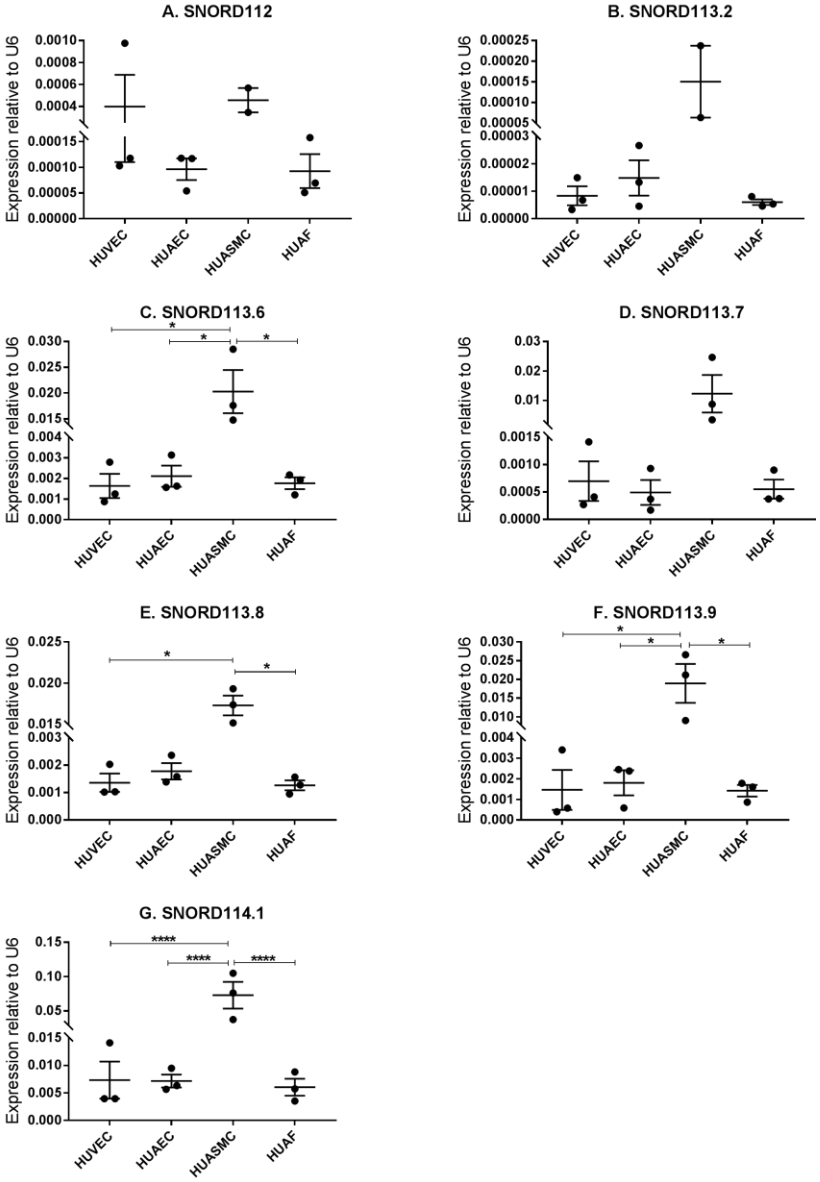

Supplemental Figure 4 Expression of 14q32 snoRNAs in primary human vascular cells. Mean values are given and errors bars represent SEMs. U6 expression was used for normalization using the $2^{-\Delta Ct}$ method. HUVEC: human umbilical venous endothelial cell; HUAEC: human umbilical arterial endothelial cell; HUASMC: human umbilical arterial smooth muscle cell; HUAF = human umbilical arterial fibroblast. * $p < 0.05$; ** $p < 0.01$ (t-test): N=3.

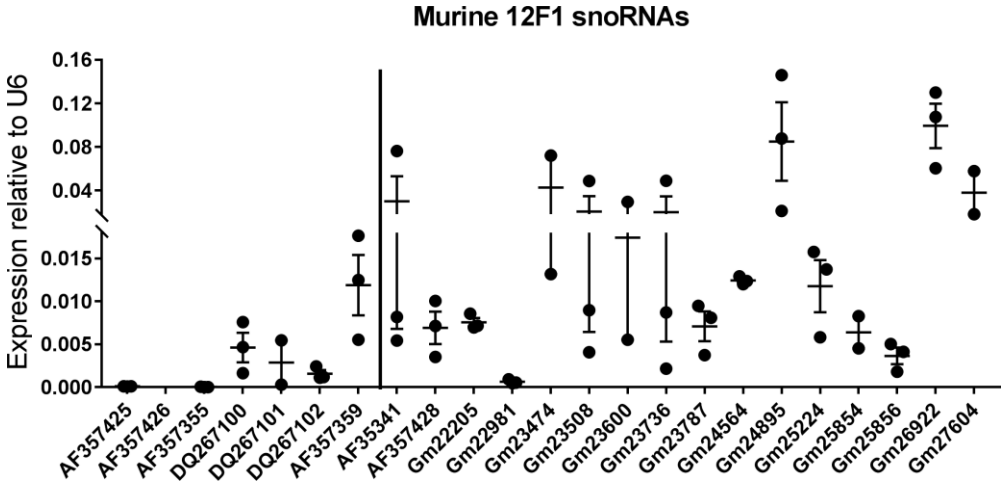

Supplemental Figure 5 Expression of annotated and predicted 12F1 snoRNAs in primary murine fibroblasts. Measurement were performed on three independent RNA isolations from independently cultured fibroblasts and errors bars represent SEMs. U6 expression was used for normalization using the $2^{-\Delta Ct}$ method. Annotated snoRNAs are depicted left of the vertical line, predicted snoRNAs are depicted right of the vertical line.

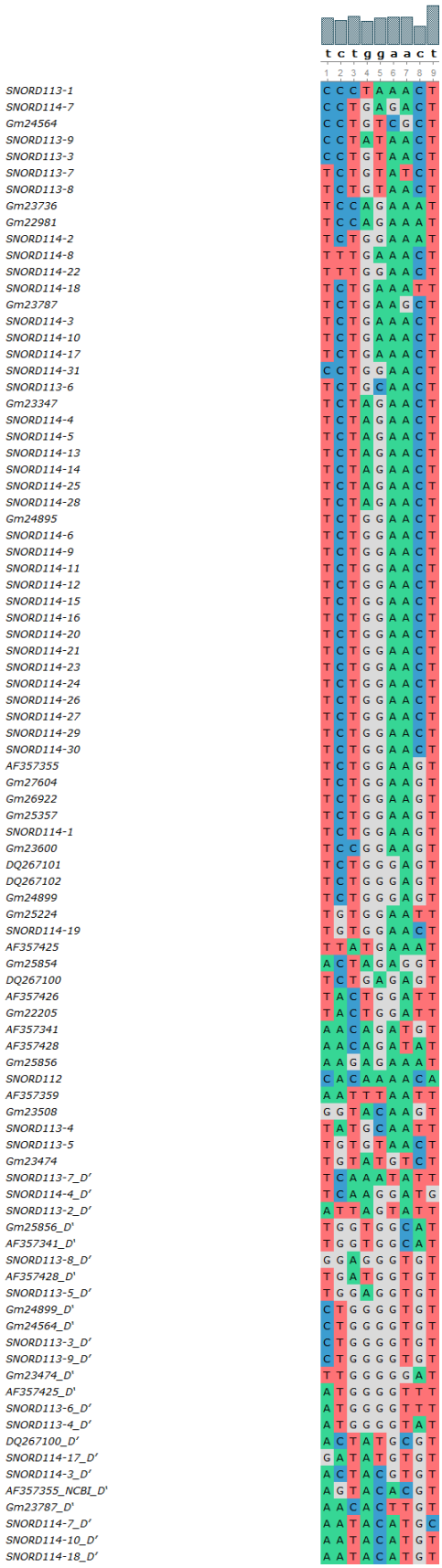

Supplemental Figure 6 Sequence-based alignment of canonical 'seed sequences'. The nine nucleotides directly upstream of C'- and D'-boxes, of human 14q32 snoRNAs (names starting with 'SNORD') and murine 12F1 snoRNAs (names starting with 'AF', 'DQ', or 'GM') are ordered based on sequence similarity.

Supplemental Table 1 Baseline characteristics of the PROSPER/PHASE study

	PROSPER/PHASE study (n=5244)
Continuous variables (mean, SD)	
Age (years)	75.3 (3.4)
Education (years)	15.1 (2.0)
Systolic blood pressure (mmHg)	154.6 (21.9)
Diastolic blood pressure (mmHg)	83.7 (11.4)
Height (cm)	165.2 (9.4)
Weight (kg)	73.3 (13.4)
Body mass index ($kg/m^{2)}$	26.8 (4.2)
Total cholesterol (mmol/L)	5.7 (0.9)
LDL cholesterol (mmol/L)	3.8 (0.8)
HDL cholesterol (mmol/L)	1.3 (0.4)
Triglycerides (mmol/L)	1.5 (0.7)
Categorical variables (n, %)	
Males	2524 (48.1)
Current smoker	1392 (26.5)
History of diabetes	544 (10.4)
History of hypertension	3257 (62.1)
History of angina	1424 (27.2)
History of claudication	354 (6.8)
History of myocardial infarction	708 (13.5)
History of stroke or TIA	586 (11.2)
History of vascular disease*	2336 (44.5)

*Any of stable angina, intermittent claudication, stroke, transient ischemic attack, myocardial infarction, peripheral artery disease surgery, or amputation for vascular disease more than 6 months before study entry.

Supplemental Table 2a All significant associations in the PROSPER/PHASE study.

Genomic Region	SNP	OR	P
Fatal or Non-Fatal Stroke and/or Coronary Events			
MEG3	rs12890215	1.136	0,04609
	rs4378559	1.135	0,0467
	rs11160607	1.133	0,04982
snoRNA	rs12879898	0.692	0,02596
Coronary Events			
DLK1	rs2273608	1,25	0,0246
MEG3	rs12431658	0,3566	0,04561
snoRNA	rs8021854	0,7249	0,02654
	rs12879898	0,6597	0,03137
	rs7159155	0,6605	0,0401
Cardiovascular Events			
MEG3	rs10144253	0,1229	0,03933
snoRNA	rs12879898	0,685	0,01651

Fatal or Non-Fatal Stroke and/or TIA			
microRNA	rs7342570	1.201	0,04927
Vascular Mortality			
snoRNA	rs2295657	1.231	0,02995
	rs12879898	0,5374	0,04767
MEG9	rs3742406	0,7996	0,01885
	rs2295655	0,7457	0,008417
	rs2295654	0,7422	0,007603
All-Cause Mortality			
MEG3	rs11160608	0,871	0,03604
	rs4906023	0,8731	0,03944
microRNA	rs11628379	0,7053	0,01991
	rs10132916	0,8514	0,03453
	rs12886869	0,8545	0,0389
	rs7161441	0,8458	0,03994
MEG9	rs2295655	0,8371	0,02158
	rs2295654	0,8337	0,01909
Hospitalization for Heart Failure			
MEG3	rs11627993	1.643	0.01165
MEG8	rs11852040	0,731	0,04402
snoRNA	rs8005672	0,7081	0,004873
	rs8017886	0,7083	0,004909
	rs4906028	0,7114	0,005507
	rs2145501	0,7128	0,006064
	rs2145504	0,6443	0,007216
	rs1125548	0,6443	0,007216
	rs11625378	0,639	0,008033
	rs12879413	0,6488	0,008168
	rs11160616	0,6512	0,00869
	rs4402490	1.299	0,01707
	rs2295657	1.286	0,01749
	rs10133948	0,7907	0,03894
	rs12433065	0,7921	0,04036
	rs11623081	0,7923	0,04062
microRNA	rs4906033	0,7314	0,01078
	rs4906034	0,7314	0,01078
	rs8003403	0,7347	0,01207
	rs8023048	0,7369	0,01298
	rs12893725	0,7612	0,02769
	rs4906032	0,784	0,03616
	rs4525426	0,7867	0,03984
	rs7342570	0,7551	0,04378
	rs6575812	0,7569	0,04711

Supplemental Table 2b Significant associations in the PROSPER/PHASE study after Correction for Multiple Testing, using False Discovery Rate (FDR; all SNPs in this table), or Bonferroni Correction (rs-numbers in bold print).

Genomic Region	SNP	OR	P	FDR-10% cut-off value for significance	Bonferroni cut-off value for significance
Hospitalization for Heart Failure					
snoRNA	**rs2145501**	0.7128	0.006064	0,0125	0,00625
	rs2145504	0.6443	0.007216	0,025	0,00625
	rs2295657	1.286	0.01749	0,0375	0,00625
	rs10133948	0.7907	0.03894	0,05	0,00625
Vascular Mortality					
MEG9	**rs2295655**	0,7457	0,00842	0,05	0,025
	rs3742406	0,7996	0,01885	0,1	0,025
All-Cause Mortality					
MEG9	**rs2295655**	0,8371	0,0216	0,05	0,025

Supplemental Table 3 Vascular tissue samples used for snoRNA analysis

	N	Mean age (SD)	Male (%)	Peri-malignancy (%)
Upper limb veins	3	51.3 (12.1)	100	0
Lower limb arteries	11	63.3 (14.0)	81.8	0
Lower limb veins	18	67.7 (13.4)	61.1	0
Abdominal arteries	14	67.6 (9.3)	64.3	64.3
Abdominal veins	5	63.0 (12.1)	80.0	60.0
Head and neck arteries	9	54.0 (28.0)	33.3	22.2
Head and neck veins	5	52.8 (18.8)	60.0	40.0
Abdominal aorta	4	65.8 (14.1)	25.0	0
Thoracic aorta	5	69.8 (16.7)	40.0	0
Mammarian arteries	18	62.0 (9.3)	72.2	0
Atrial appendage	1	50 (-)	100	0
Radial artery	1	42 (-)	100	0
Umbilical artery	1	0 (-)	unknown	0
Total	95	61.8 (16.5)	63.2	16.8

Supplemental Table 4 3GA Sequences.

Oligonucleotide	Sequence
3GA-Control	3’-TGTACGACTCCATAACGGT-X-TGGCAATACCTCAGCATGT-3’
3GA-AF357425	3’-GGGTTTAATCACTGTCCTC-X-CTCCTGTCACTAATTTGGG-3’
3GA-AF357426	3’-AGTATGTTGTCATCGTCTA-X-ATCTGCTACTGTTGTATGA-3’
3GA-DQ267100	3’-ACCTCAGACTCTCAGACGC-X-CGCAGACTCTCAGACTCCA-3’
3GA-DQ267101	3’-TGGAACTCAGACTCCCAGA-X-AGACCCTCAGACTCAAGGT-3’
3GA-AF357355	3’-TGAATCTCAGACTTCCAGA-X-AGACCTTCAGACTCTAAGT-3’
3GA-DQ267102	3’-ACCTCAGACTCCCAGACCT-X-TCCAGACCCTCAGACTCCA-3’

‘X’: Phosphorothioate linker

‘NNN’: 2’-O-methyl-modified DNA nucleotides

Supplemental Table 5 qPCR Primer Sequences

Oligonucleotide	Sequence
sno112.FW	TGGACCAATGATGAGACAGTG
sno112.Rev	GTGCAGAACTGGATTAATCATG
sno113.2-FW	TAGCCAATCATTAGTATTCTGAGC
sno113.2-Rev	AACCTCTGAGTTACAGAATCTA
sno113.6-FW	TGGACCAGTGATGAATATCATG
sno113.6-Rev	TGGACCTCAGAGTTGCAGATG
sno113.7-FW	TGGATCAATGATGAGTATGCGT
sno113.7-Rev	GACCTCAGAGATACAGACAGG
sno113.8-FW	TGGACCAATGATGAGATTGG
sno113.8-Rev	GGACCTCAGAGTTACAGATGGC
sno113.9-FW	GGATCAATGATGAGTACCCTG
sno113.9-Rev	TGGACCTCAGAGTTATAGGG
sno114.1-FW	GGACCTATGATGATGACTGG
sno114.1-Rev	TGGACCTCAGACTTCCAGACC
DQ267100-FW	CAATGATGACTGTGGGTGCT
DQ267100-RV	CCTCAGACTCTCAGACGCATA
DQ267102-FW	GATGACCTCTGGTGCCGTAT
DQ267102-RV	TGGACCTCAGACTCCCAGAC
DQ267101-FW	TCAATGATGACCAGCGGTAG
DQ267101-RV	TGGAACTCAGACTCCCAGAT
AF357426-FW	TGACCTTGTCTATATTATAAGTCAT
AF357426-FW	ACCTCAGAATCCAGTATGTTGTCA
AF357355-FW	GGGTGGGTTATGAGTTGTGG
AF357355-RV	TCTCAGACTTCCAGACATGTACTCA
AF357425-FW	AGGAGCATGGGGTTTCTGAC
AF357425-RV	TTTCATAAGGGTTTAATCACTGTCC
Gm26922_FW	ACAAAGGGTGGCGTATGAGT
Gm26922_RV	TCAGACTTCCAGACATGTACTCA

AF357428_FW	AGGACCGATGATGAGATCTGA
AF357428_RV	TGTTCATGTCATCGAGAAACACT
AF357341_FW	ATCTGGTGGCATCTGACTGT
AF357341_RV	GACATCTGTTCTCATGGCTGT
Gm23508_FW	CCTCTGGTAGCACACGATTTG
Gm23508_RV	CAGACTTCCAGACCTGTACCC
Gm25224_FW	TGATGACTCTGGTGGTGTGG
Gm25224_RV	GGACCTGAGAATTCCACATATGC
Gm23600_FW	AATGATGGCCAGTGATGATGT
Gm23600_RV	GACGACCAGACCTGTAGCTA
Gm23736_FW	TGATGAGATCTGGTGGCGTT
Gm23736_RV	GGATACTTGGCGTTCATGGAG
Gm23474_FW	TCAGTGAGGAGAACTTGGGG
Gm23474_RV	GACCTCAGAGACATACATGGGT
Gm27604_FW	TCTTGTTGGAGGTGAGCAGT
Gm27604_RV	CTCAGACTTCCGGACCTGTT
Gm24564_FW	CTGACCAATGATGAGAATTCTGG
Gm24564_RV	AGCGACAGGGTTAATCATAATCA
Gm24895_FW	GGCCAATGATGACGAGGTTT
Gm24895_RV	TGGACCTCAGACCTCTAGTGA
Gm25854_FW	ACCGGTGGCATTTGACTCAT
Gm25854_RV	GGATCTTGGTGTTTCAGACTCA
Gm22205_FW	TGACTGATCCTGAGCACTGT
Gm22205_RV	AGATCTCAAAGTTCCAGACATGT
Gm25856_FW	CAATGATGAGATCTGGTGGCA
Gm25856_RV	AGATTTCTCTTGACATGGATGCC
Gm22981_FW	GGACCGATGATGAGATCTGG
Gm22981_RV	TTCTGGATACTTGGCGTTCA
Gm23787_FW	CCAAGGTATGAGAGAGATGACG
Gm23787_RV	GGACCTCTGAGCTTCAGACAA
U6-FW	AGAAGATTAGCATGGCCCCT
U6-RV	ATTTGCGTGTCATCCTTGCG
GAPDH-FW	CACCACCATGGAGAAGGC
GAPDH-RV	AGCAGTTGGTGGTGCAGGA

Supplemental Table 6 Associations of SNPs, inside 14q32 gene regions, with CAD in the Cardiogram Meta-Analysis.

Genomic Region	SNP	Log Odds (OR)	P
DLK1	rs1555406	0,0510275 (1,124676187)	0,020927
IG-DMR	rs12437020*	-0,039967 (0,912080981)	0,037739
RTL1/ MIR493-MIR136	rs4906018	0,0389087 (1,093726412)	0,018723
	rs1077411*	0,0495353 (1,120818524)	0,037604
	rs1077412*	0,0612703 (1,151516857)	0,02932
snoRNA	rs1956734*	-0,041743 (0,908357487)	0,016671
	rs2295657*	-0,038137 (0,915931299)	0,019897
	rs10135691	0,0487901 (1,118896976)	0,031895
	rs4402490	0,034168 (1,081852368)	0,03986
	rs12879898	-0,050005 (0,891240267)	0,049692
MEG9	rs2007291	0,039289 (1,094684579)	0,022437

*Also associates with cardiovascular endpoints in PROSPER